# POLYMERIC NANOCOMPOSITES FROM RENEWABLE RESOURCES

by

Esra Altuntaş

B.S., Chemistry, Hacettepe University, 2005

Submitted to the Institute for Graduate Studies in
Science and Engineering in partial fulfillment of
the requirements for the degree of
Master of Science

Graduate Program in Chemistry

Boğaziçi University

2008

**To My Family**

# ACKNOWLEDGEMENTS

I would like to express my most sincere gratitude to my thesis supervisor Prof. Dr. Nihan Nugay for her helpful supervision, endless attention, most valuable encouragement and scientific guidance throughout my thesis study. I wish to express my great appreciation to Prof. Dr. Turgut Nugay, for sharing his ideas, most valuable comments during this study. I greatly appreciate to both of them for their suggestions and continued support.

I wish to thank to the members of my thesis committee: Prof. Dr. Selim Küsefoğlu, and Prof. Dr. Yusuf Yağcı for making helpful comments.

I am especially grateful to my laboratory colleagues Dr. Sinan Şen, and Çimen Özgüç for their invaluable helps. I would like to express special thanks to Gökhan Çaylı for his most valuable help during this study. I wish to thank to Dr. Bilge Gedik Uluocak, and Aslı Çakır for characterizing the products of this study. I also would like to thank Işıl Nugay for her help during the preparation of LB medium.

I also would like to thank to all my friends in the Department of Chemistry, for their support and friendship.

Finally, I would like to express my indepthness gratitude and love to my father, my mother, and my brother for their continuous moral support, love, encouragement, and understanding throughout these years.

# ABSTRACT

## POLYMERIC NANOCOMPOSITES FROM RENEWABLE RESOURCES

Objective of this study was to synthesize renewable polymeric nanocomposites by using an in-situ polymerization method and characterize them in terms of thermal and mechanical properties as well as morphology. Firstly, renewable soy bean oil based intercalant was synthesized, and it is characterized by HNMR and FTIR techniques. By using this intercalant which is quarternized derivative of acrylated epoxidized soy bean oil (AESO), modification of montmorillonite (MMT) was completed. The characterization of modified montmorillonite (m-MMT) was performed via X-ray diffraction (XRD) and Thermogravimetric Analysis (TGA). In the second step, the synthesis of renewable polymeric nanocomposites from acrylated epoxidized soy bean oil (AESO), styrene (as a diluent) and modified montmorillonite (m-MMT) was achieved and the effect of increased nanofiller loading in mechanical and thermal properties of acrylated epoxidized soy bean oil (AESO) nanocomposites were analyzed by Dynamic Mechanical Analyzer (DMA), Differential Scanning Calorimeter (DSC) and Thermogravimetric Analysis (TGA). In the third step, the characterization studies of the acrylated epoxidized soy bean oil nanocomposites were completed by using X-ray diffraction (XRD), Atomic Force Microscopy (AFM) and Scanning Electron Microscopy (SEM) techniques. Desired exfoliated structure was achieved by using modified montmorillonite (m-MMT) in this kind of renewable polymeric nanocomposites. Resultant delaminated nanocomposites were found to have significant improvements both in thermal stability and dynamic mechanical performance as compared with virgin acrylated epoxidized soy bean oil based polymers even with one per cent of clay loading. Finally, biodegradability studies of the nanocomposites were done by using soil burial method and it was found that all resultant nanocomposites were biodegradable in soil and it was found that increasing the clay content increase the biodegradability of the nanocomposites. In order to confirm biodegradability studies, Lysogeny broth medium was used, and it was found that resultant nanocomposites were not antibacterial and bacteria species could easily promote their growth on these nanocomposites.

# ÖZET

## YENİLENEBİLİR KAYNAKLI POLİMERİK NANOKOMPOZİTLER

Bu çalışmada amaç in-situ polimerizasyon yöntemiyle tamamıyle yenilenebilir kaynaklardan polimerik nanokompozitler sentezlemek ve elde edilen nankompozitleri termal, mekanik ve morfolojik özellikleri açısından incelemektir. İlk olarak, soyayağı bazlı interkelant sentezledikten sonra, bu Akrilatlanmış Epokside edilmiş soya yağının kuarternize edilmiş türevi kullanılarak MMT kilinin modifikasyonu tamamlanmıştır. Modifiye edilmiş kilin karakterizasyonu XRD (X-ışını Saçınımı) ve TGA (Termal Gravimetrik Analiz) kullanılarak yapılmıştır ve modifikasyon ispatlanmıştır. İkinci aşamada, yenilenebilir kaynaklardan polimerik nanokompozit sentezi AESO, stiren ve modifiye-MMT kullanılarak tamamlanmıştır ve nanodolgu miktarının nanokompozitlerin termal ve mekanik özelliklerine olan etkisi DMA (Dinamik Mekanik Analiz), DSC (Diferansiyel Taramalı Kalorimetre) ve TGA (Termal Gravimetrik Analiz) analizleri kullanılarak tespit edilmiştir. Üçüncü aşamada, XRD (X-ışını Saçınımı), AFM (Atomik Kütle Mikroskobu), ve SEM (Taramalı Elektron Mikroskobu) analiz metodları kullanılarak elde edilen AESO bazlı nanokompozitlerin morfolojik özellikleri belirlenerek karakterizasyon çalşımaları tamamlanmıştır. İstenilen eksfoliye olmuş nanokompozitler modifiye-MMT kilinin kullanımı ile elde edilmiştir. Elde edilen delamine olmuş nanokompozitlerin termal kararlılık ve dinamik mekanik performans olarak kendilerinin AESO bazlı saf matriks polimerlerine göre sadece yüzde bir dolgu kullanıldığında bile belirgin bir biçimde daha iyi oldukları belirlenmiştir. Son olarak, yenilenebilir kaynaklardan elde edilmiş bu nanokompozitlerin biyobozunurluk testleri toprağa gömme metodu ile yapılmıştır ve artan kil miktarının nanokompozitlerin biyolojik bozunmalarını arttırdığı bulunmuştur. Lysogeny ortamı kullanılarak biyobozunurluk testlerinin doğruluğu bir kez daha ispatlanmıştır. Sonuç olarak bu nanokompozitlerin antibakteriyel olmadığı ve bakteri türlerinin gelişimlerini kolay bir şekilde bu nanokompozitlerin üzerinde gerçekleştirdiği belirlenmiştir.

# TABLE OF CONTENTS

# LIST OF FIGURES

# LIST OF TABLES

# LIST OF SYMBOLS/ABBREVIATIONS

| | |
|---|---|
| AESO | Acrylated Epoxidized Soybean Oil |
| AFM | Atomic Force Microscopy |
| DMA | Dynamic Mechanical Analysis |
| DSC | Differential Scanning Calorimetry |
| E’ | Storage Modulus |
| E” | Loss Modulus |
| ESO | Epoxidized Soybean Oil |
| FA | Furfuryl Amine |
| LB | Lysogeny Broth |
| ml | Millilitre |
| MMT | Montmorillonite |
| SEM | Scanning Electron Microscopy |
| SO | Soybean Oil |
| TGA | Thermogravimetric Analysis |
| THF | Tetrahydrofuran |
| XRD | X-Ray Diffraction |

# 1. INTRODUCTION

## 1.1. Polymeric Nanocomposites

Composites are engineered materials made from two or more constituent materials with significantly different physical and chemical properties and which remain separate and distinct on a macroscopic level within the finished structure. In composite structure, there are two categories of constituent materials: matrix and reinforcement. At least one portion of each type is required. The matrix material surrounds and supports the reinforcement materials by maintaining their relative positions. The reinforcements import their special mechanical and physical properties to enhance the matrix properties. A synergism produces material properties unavailable from the individual constituent materials, while the wide variety of matrix and strengthening materials allows the designer of the product or structure to choose an optimum combination.

Nanocomposites are materials that are crated by introducing nanoparticulates (fillers) into a macroscopic sample material (matrix). After adding the nanoparticulates to the matrix material, the resulting nanocomposites may exhibit drastically enhanced properties.

Polymeric nanocomposites consist of a polymer matrix resin and inorganic particle that has at least one dimension in the nanometer scale such as layered silicates. A large number of polymers are filled with layered silicates in order to improve the stiffness and toughness of the materials, to enhance their barrier properties and their resistance to fire and ignition or basically decrease cost [1].

Polymer/layered silicate nanocomposites have attracted great interest because of their significant improvement in mechanical and thermal properties when compared with virgin polymer or conventional micro and macro composites [2]. Increased moduli, strength, and heat resistance, decreased gas permeability and flammability are the other improved properties.

Nanocomposite material was firstly discovered by Toyota research group who synthesized a nanostructure from a polymer and an organophilic layered silicate. This new material, based on polyamide 6 and organophilic montmorillonite clay, showed dramatic improvements in mechanical properties, barrier properties, and heat distortion temperature, even at very low content of layered silicate (4 per cent by weight)[3].

According to method of preparation and the nature of the components used, three main types of composites can be obtained when a layered silicate is associated with a polymer. Micro composite (phase separated) (a) is obtained when the polymer chains are unable to intercalate between the layers of the silicate particles. Intercalated nanocomposite (b) is formed when one or more extended polymer chains distributed between the layered silicates as a result in a well ordered multilayer morphology. Therefore, the interlayer spacing is increased but the ordered layer structure of the layered silicates is retained. Exfoliated or delaminated structure (c) is formed when the layered silicates are completely and uniformly distributed in a polymer matrix [1].

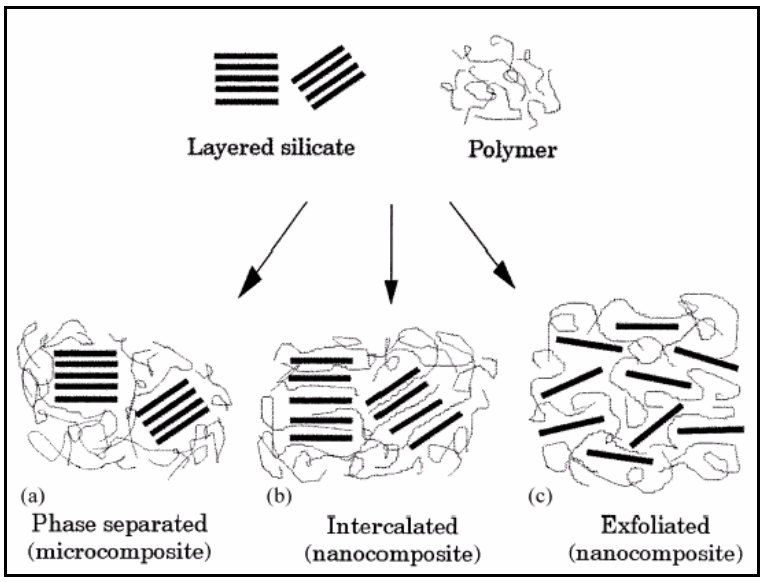


Figure 1.1 Different types of polymer-clay nanocomposites [1]

## 1.2. Materials Used in Nanocomposite Synthesis

### 1.2.1. Layered Silicates

Inorganic layered materials exist in great variety and they possess well defined, ordered intralamellar space potentially accessible by foreign species. This ability enables them to form hybrid nanocomposite materials. The layered silicates are commonly used in preparation of polymer/layered silicate nanocomposites belong to the structural family of 2:1 phyllosilicates. (Table1.1) [1-4]. Their crystal lattice consists of two dimensional layers where a central octahedral sheet of alumina or magnesia is fused to two external silica tetrahedron by the tip so that the oxygen ions of the octahedral sheet do also belong to the tetrahedral sheets. The layer thickness is around 1 nanometer (nm) and the lateral dimensions of these layers may vary from 300 Å to several microns or larger, depending on the particular layered silicate. These layers organize themselves to form stacks with a regular van der Waals gap between them. This gap is called the interlayer or the gallery. Isomorphic substitution within the layers; $Al^{+3}$ replaced by $Mg^{+2}$ or $Fe^{+2}$, or $Mg^{+2}$ replaced by $Li^{+}$ , generates negative charges that are counterbalanced by alkali or alkaline earth cations situated inside the galleries. As the forces that hold the stacks together are relatively weak, the intercalation of small molecules between the layers is easy [4].

Table 1.1 Chemical structures of 2:1 phyllosilicates [4]

| 2:1 phyllosilicate | General formula |
|---|---|
| Montmorillonite | $M_x[Al_{4-x}Mg_x](Si_8)O_{20}(OH)_4$ |
| Hectorite | $M_x[Mg_{6-x}Li_x](Si_8)O_{20}(OH)_4$ |
| Saponite | $M_x[Mg_6]\ (Si_{8-x}Al_x)O_{20}(OH)_4$ |
| M = monovalent charge compensating cation in the interlayer<br>x = degree of isomorphous substitution (between 0.5-1.3) | |

Montmorillonite (MMT) is the most commonly used layered silicate as nanofiller due to its suitable layer charge density. The structure of montmorillonite is shown in Figure 1.2 [5].

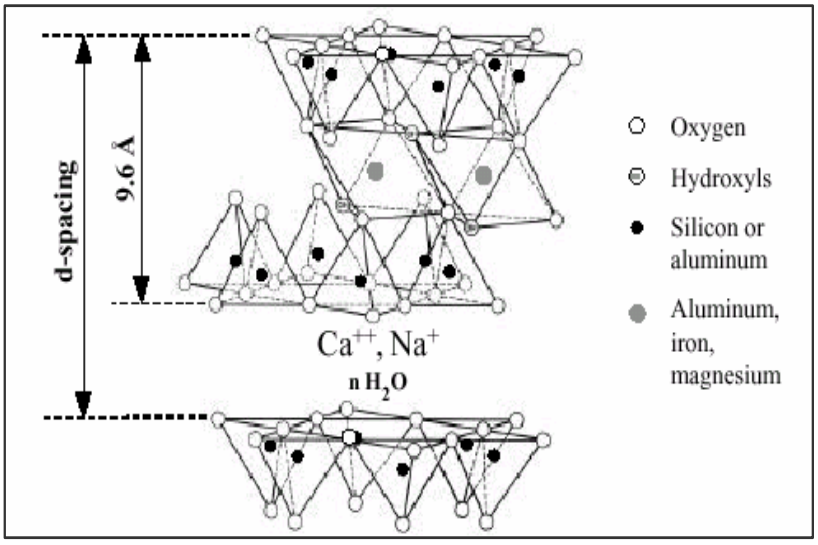


Figure 1.2 Idealized structure of montmorillonite, proposed by Hoffman, Endell and Wilm, [5] showing two tetrahedral sheets fused to one octahedral sheet

In nanocomposite synthesis, there is an important challenge to increase interlayer distance and to reduce electrostatic interlayer interactions in order to promote in-situ nanoparticle formation. Properties of nanocomposite depend on the degree of nanoclay deagglomeration and dispersion within the polymer matrix. The most important factor which influences delamination/exfoliation and intercalation of clay with polymer is the nanoclay surface treatment. Therefore, it is very important to modify layered silicate in order to disperse it in polymer matrix.

### 1.2.2. Compatibilizing Agents

Dispersing layered silicates in an organic polymer matrix is usually very difficult due to the hydrophilicity of montmorillonite and other layered silicate. Hydrophilic behavior makes them poorly suited to mixing and interacting with most polymer matrices. Also, the stacks of clay platelets are held tightly together by electrostatic forces and counterions are attracted to the net negative charge within the clay platelets. The counterions can be shared by two neighboring platelets, resulting in stacks of platelets that are tightly held together. For these reasons, the clay must be pre-treated before it can be used to make a

nanocomposite, so a compatibilizing agent is required and it is typically a molecule with one hydrophilic and one organophilic function. The most commonly used method of modifying the clay surface, making it more compatible with an organic polymeric matrix, is ion exchanging.

The ability to sorb certain cations and to retain them in an exchangeable state is a characteristic feature of montmorillonite (MMT). $Na^{+}$, $Ca^{+2}$, $Mg^{+2}$, $H^{+}$, $K^{+}$, and $NH_4^{+}$ are the most common exchangeable cations, these cations are not strongly bound to the clay surface, therefore these small molecule cations can be replaced with cations which can present on the clay.

For a given clay, the maximum amount of cations that can be taken up is constant and is known as the cation exchange capasity (CEC). It is measured in miliequivalents per gram (meq/g) or more frequently per 100 (meq/100g). By exchanging with various organic cations, montmorillonite (MMT) clay can be compatibilized with a wide variety of matrix polymers. Therefore, this process helps to separate the clay platelets so that they can be more easily intercalated and exfoliated [1].

Amino acids are the first compatibilizing agents used in the synthesis of polyamide-6-clay hybrids [3]. The most commonly used compatibilizing agents are alkyl ammonium ions because they can be easily exchanged with the inorganic ions situated in the galleries between the silicate layers. The cation-exchange process of linear alkyl ammonium ions is described in Figure 1.3 [6].

In order to facilitate both the matrix and silica layers compatibilization and the diffusion of the monomer or polymer chains into interlayer galleries which results in delamination, montmorillonites have mostly been treated with quarternized alkyl ammonium salts containing heavy structures both in the form of oligomers, polymers, and copolymers [7-9].

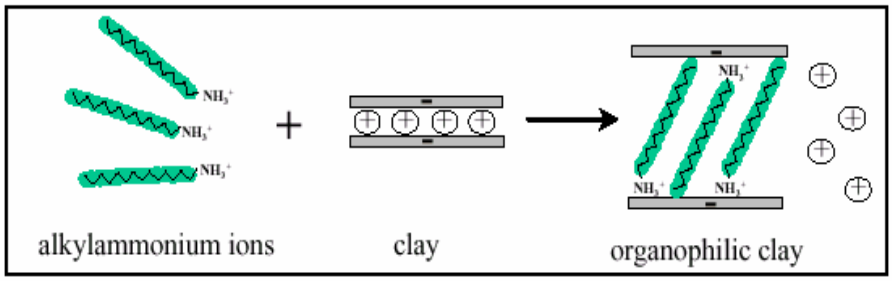


Figure 1.3 The cation-exchange process between alkyl ammonium ions and cations initially intercalated between the clay layers [6]

The organically modified layered silicate (or organoclay) being organophilic, its surface energy is lowered and it is more compatible with organic polymers. So, in order to use inorganic montmorillonite (MMT) clay in nanocomposites synthesis, compatibilizing agents have to be used to modify this layered silicate.

### 1.2.3. Polymers Used in Nanocomposites

Every kind of polymers, including thermoplastics and thermosets, can be used in polymeric nanocomposite synthesis. Many different polymers have already been used to synthesize polymer/layered silicates nanocomposites. Polyamide 6 has been the first and the most studied thermoplastic for the synthesis of polymer/layered silicates nanocomposites [10-11]. Other thermoplastics such as poly (ethylene oxide) [12], poly (methyl methacrylate) [13], poly (butadiene acrylonitrile) [14], poly (ε-caprolactone) [15], polystyrene [16-17], polyimide [18-19] and poly (ethylene terephthalate) [20] have since been used to synthesize polymer/layered silicates nanocomposites by different methods. Thermoset polymers have also been used to synthesize polymer/layered silicates nanocomposites. Epoxy-clay nanocomposites have been extensively studied [21-23]. Nanocomposites based on polyurethanes [24-25] and silicone rubbers [26-27] have also been reported in the literature.

Most of the monomers of these polymers are petroleum based, and petroleum based resources are depleted speedily and the prices of these resources increases continuously. So

there is a need to use cheaper and renewable resources instead of petroleum based resources. Because of this reason, in the last years, many research efforts have been done to synthesize green polymeric nanocomposites from different renewable resources such as oil based resources.

## 1.3. Synthesis of Polymer-Clay Nanocomposites

The polymer/layered silicates nanocomposites have been synthesized by using three different methods, in-situ polymerization method, solution polymerization method, and melt intercalation method.

### 1.3.1. In-situ Polymerization

In-situ polymerization was the first method used to synthesize polymer-clay nanocomposite. In this method, firstly the layered silicate is swollen within the liquid monomer or a monomer solution so the polymer formation can occur between the intercalated sheets. This step requires a certain amount of time, which depends on the polarity of the monomer molecules, the surface treatment of the organoclay, and the swelling temperature. Polymerization can be initiated either by heat or radiation, by the diffusion of a suitable initiator, or by an organic initiator [2].

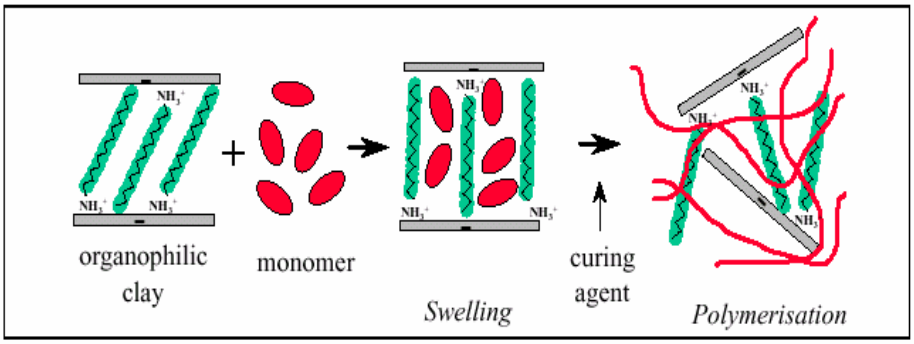


Figure 1.4 The in-situ polymerization technique. [23]

The driving force of the “in situ-polymerization” method is linked to the polarity of the monomer molecules and is believed that during the swelling phase, the high surface energy of the clay attracts polar monomer molecules so that they diffuse between the clay layers. When certain equilibrium is reached the diffusion stops and the clay is swollen in the monomer to a certain extent corresponding to a perpendicular orientation of the alkyl ammonium ions. When the polymerization is initiated, the monomer starts to react with the curing agent. This reaction lowers the overall polarity of the intercalated molecules and displaces the thermodynamic equilibrium so that more polar molecules are driven between the clay layers. As this mechanism occurs, the organic molecules can delaminate the clay.

### 1.3.2. Solution Method

Intercalated polymer/layered silicates nanocomposites can be synthesized by using polar solvents. This method is similar to the one used in the in-situ polymerization method. Firstly, the organoclay is swollen in the solvent. Then, the polymer which is dissolved in the same solvent is added to the solution and intercalates between the clay layers. Finally, the solvent is removed by evaporation usually under vacuum.

### 1.3.3. Melt Intercalation Method

In this method, the layered silicate is mixed with the polymer matrix in the molten state. The mixture is then annealed at a temperature above the glass transition temperature of the polymer and forms a nanocomposite. No solvent is required in this method. Under these conditions and if the layer surfaces are sufficiently compatible with the chosen polymer, the polymer can diffuse into the interlayer space and form either an intercalated or an exfoliated nanocomposite [4]. The polymer chains lose conformational entropy during the intercalation. The proposed driving force for this mechanism is the important enthalpic contribution of the polymer/organoclay interactions during the blending and annealing steps. Many polymer/organosilicate hybrids obtained by melt intercalation have been investigated in recent years.

### 1.4. Characterization of Polymer-Clay Nanocomposites

Two different methods are mainly used to characterize the structure of polymer/layered silicate nanocomposites, which are X- Ray Diffraction (XRD) and Transmission Electron Microscopy (TEM). X- Ray Diffraction (XRD) analysis is generally used to identify the nanocomposite structure by monitoring the position, shape, and intensity of the basal reflections from the distributed silicate layers, because it is a good way to evaluate the spacing between the clay layers and their relative stacking order. The interlayer distance and stacking order determine the structure (intercalated or exfoliated) and the performance of nanocomposites.

The intercalation of polymer chains and organophilic modification of layered silicate usually increases the interlayer spacing (d-spacing), in comparison with the spacing of the organoclay used leading to a shift of the diffraction peak towards lower angle values. Bragg's rule [4] is used to calculate angle and layer spacing values as expressed in Equation (1.1):

$$n\lambda = 2.d.\sin\theta$$

where $\lambda$ corresponds to the wavelength of the x-ray radiation used in the diffraction experiment, d is the spacing between the diffractional lattice planes and $\theta$ is the measured diffraction angle.

In the exfoliated nanocomposites, the extensive layer separation associated with the delamination of the original silicate layers in the polymer matrix results in the eventual disappearance of any coherent X-ray diffraction from the disturbed silicate layers.

X- Ray Diffraction (XRD) has some disadvantages that X- Ray Diffraction (XRD) can not differentiate between certain types of clay dispersions found in polymers. In exfoliated structure, no more diffraction peaks are visible in the X-ray diffractograms either because of a much too large spacing between the layers (i.e. exceeding 8 nm in the case of ordered exfoliated structure) or because the nanocomposite does not present ordering anymore.

Another technique which is used to characterize nanocomposites morphology is Transmission Electron Microscopy (TEM). TEM can be used to confirm results obtained by XRD about the organization of the clay layers in the nanocomposite. It can be found by TEM whether the structure is intercalated or exfoliated. Besides these two well defined structures, other intermediate organizations can exist presenting both intercalation and exfoliation. In this case, a broadening of the diffraction peak is often observed and one must rely on TEM observation to define the overall structure [4].

### 1.5. Properties of Polymer-Clay Nanocomposites

Polymer/layered silicate nanocomposites have broaden their applications in many fields with their physical and chemical properties with loading of nanometer-sized particles; these materials have shown enhanced mechanical properties, such as increased stiffness, strength, thermal stability, flame retardancy and gas barrier properties with respect to virgin polymer matrix [28]. The main reason for these improved properties is the stronger interfacial interaction between the matrix and layered silicate, compared with conventional filled-reinforced systems.

Presence of nanometer scale fillers in the polymer matrix increases the mechanical properties of nanocomposite significantly compared to virgin polymer. Mechanical properties of the nanocomposites are tested by Dynamic Mechanical Analysis (DMA) whose results are expressed by three main parameters: (a) the storage modulus (E') corresponding to the elastic response to the deformation; (b) the loss modulus (E") corresponding to the plastic response to the deformation and (c) tan δ, that is the (E'/E") ratio, useful for determining the occurrence of molecular mobility transitions such as the glass transition temperature. The modulus of the polymer/layered silicate nanocomposites depends on the degree of exfoliation of the layered silicate in the polymer.

In general, tensile elongation of conventional polymer-inorganic filler composites is low. On the other hand, the nanocomposite exhibits as large an elongation as over 100 percent when its thickness is less than 1mm. This property enables the nanocomposites to be converted to fibers and films. The tensile modulus of a polymeric material has been showed to be improved when nanocomposites are formed with layered silicates [29]

The thermal stability of nanocomposites are highly increased with respect to pure polymer matrix was found to enhance thermal stability by acting as superior insulator and mass transport barrier to the volatile products generated during decomposition. [2]

Another highly interesting property exhibited by polymer/layered silicate nanocomposites concerns their unique ability to promote flame retardancy at quite low filling level through the formation of insulating and incombustible char.

Clays are believed to increase the barrier properties by creating a maze or "tortuous path" that retards the progress of the gas molecules through the matrix resin. The direct benefit of the formation of such a path is observed in some nanocomposites by dramatically improved barrier properties with a simultaneous decrease in the thermal expansion coefficient [30]

Another interesting and exciting aspect of nanocomposite technology is the significant improvement in the biodegradability after nanocomposite preparation with organically modified layered silicate.

### 1.6. Applications of Polymer-Clay Nanocomposites

Nanocomposites have many applications due to the property advantages that nanomaterial additives can provide in comparison to both their conventional filler counterparts and base polymer. Properties which have been shown to undergo substantial improvements include:

- Mechanical properties e.g. strength, modulus and dimensional stability
- Decreased permeability to gases, water and hydrocarbons
- Thermal stability and heat distortion temperature
- Flame retardancy and reduced smoke emissions
- Chemical resistance
- Surface appearance
- Electrical conductivity

– Optical clarity in comparison to conventionally filled polymers

Such mechanical property improvements have resulted in major interest in nanocomposite materials in numerous automotive and general/industrial applications. These include potential for utilization as mirror housings on various vehicle types, door handles, engine covers and intake manifolds and timing belt covers. More general applications currently being considered include usage as impellers and blades for vacuum cleaners, power tool housings, mower hoods and covers for portable electronic equipment such as mobile phones, pagers etc.

Renewable polymeric nanocomposites are especially very important for food packaging applications. It is likely that excellent gaseous barrier properties exhibited by nanocomposite polymer systems will result in their substantial use as packaging materials in future years.

## 1.7. Renewable Resources for Nanocomposite Synthesis

### 1.7.1. Plant Oils.

Plant oils are composed of three fatty acid chains joined by a glycerol unit. The fatty acids may be saturated or may contain one, two, or three unsaturations. The double bonds are isolated and in the cis geometry. The length of the fatty acid chains vary from 14 to 22 carbons. There are also some rare triglycerides containing unusual functionalities, such as hydroxyls, epoxies, cyclic groups, and furanoid groups.

Figure 1.4 shows the general representation of a triglycerides molecule. x, y, and z groups (R1, R2 and R3) represent long alkyl chains with varying functionalities. The functionality of fatty acid varies depending on the type of plant from which the oil is obtained.

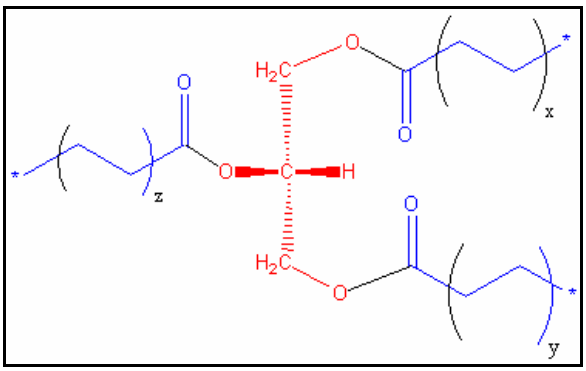


Figure 1.5 General structure of triglyceride

### 1.7.1.1 Soybean Oil.

Soybean is one of the oldest crops cultivated by humans, and it is grown in over 50 countries, but mostly in the USA, China, Brazil, and Argentina. Soybean oil shows wide variation in composition, but it is mainly composed of triglycerides of oleic and linoleic acids [31].

The triglycerides molecules of soybean oil contain four different reactive sites. Figure 1.5 shows all active sites, which are capable of doing chemical reactions: (1) allylic carbon, (2) double bond, (3) the carbons alpha to the ester group, and (4) ester group. These reactive sites on the triglyceride molecules are used to introduce polymerizable groups by using the some procedures that have been applied in the synthesis of petroleum based polymers.

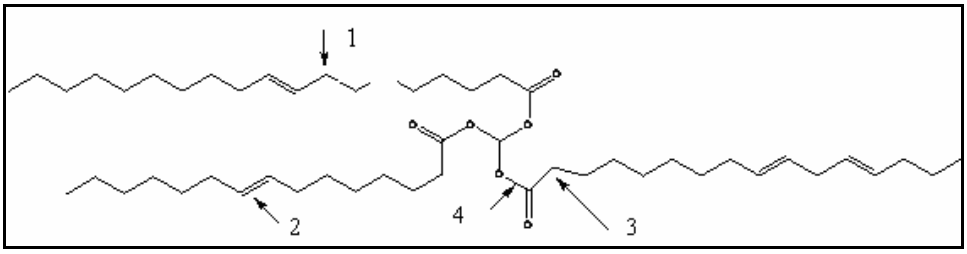


Figure 1.6 Reactive sites of a triglyceride molecule

**1.7.1.2 Acrylated Epoxidized Soybean Oil.**

Soybean oil is firstly epoxidized to obtain Epoxidized Soybean oil (ESO). Epoxidation is the most important reactions at the double bond of unsaturated fatty acids, and then a standard substitution reaction is used in the mechanism of the reaction of ESO in order to obtain AESO. The following figure shows the structure of Acrylated Epoxidized Soybean oil (AESO).

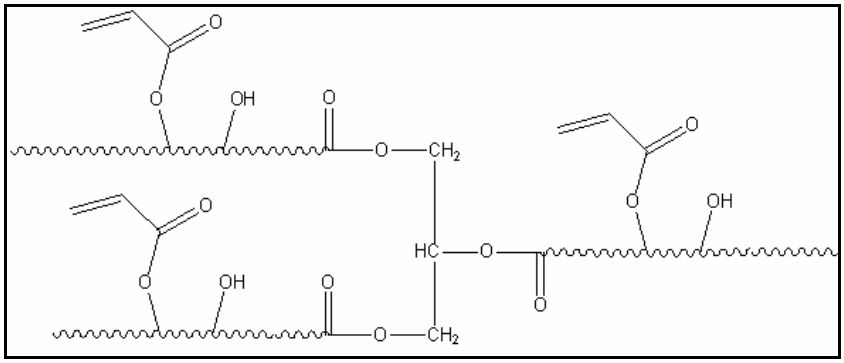


Figure 1.7 Structure of AESO

Acrylated Epoxidized Soybean oil (AESO) can be polymerized by using free radical polymerization with reactive diluents such as styrene, to give thermoset resins, which will give mechanical properties similar to commercial successful polyester and vinyl ester resins [32]. Polymer properties can be controlled by changing the functionality of the molecule such as acrylate groups on Acrylated Epoxidized Soybean oil (AESO). AESO based polymers with different moduli and glass transition temperatures (Tg) can be produced by varying the amount of reactive diluents.

## 1.8. Renewable Polymeric Nanocomposites

Petroleum based raw materials have been the most commonly used resources in the synthesis of polymeric materials for the last 50 years. The depletion in the petroleum reserves and the increase of the petroleum price have been driven the chemical industry to search for new resources. So, there is a great need of renewable resources which have ways

of regenerating themselves as they are depleted. These resources are mostly preferred by the industry due to their prices and renewable characteristic. Renewable resources for polymeric materials provide an alternative to maintaining sustainable development of ecologically and economically attractive technology. The developments of materials from biodegradable polymers, the preservation of petroleum based resources, complete biologically degradability, the decrease in the volume of garbage and combustibility in the neutral cycle, protection of the climate through the reduction of carbon dioxide released, also the application possibilities of agricultural resources for the production of green materials are some of the reasons why renewable biodegradable polymers and polymeric nanocomposites have attracted the academic and industrial interest.

Renewable feedstocks are an available and useful substitute for petrochemical feedstocks because the prices increase in oils. They can improve waste disposal methods, and reduce the use of landfill sites. Renewable resources can be used in packaging applications and they can replace petrochemicals in the manufacture of polyesters and polyurethanes, for use in foams, textiles, etc.

Renewable resources-based biodegradable polymers so far used for the preparation of nanocomposites are polylactide (PLA), poly (3-hydroxy butyrate) (PHB) and its copolymers, thermoplastic starch, plant oils and their functionalized derivatives, cellulose, gelatine, chitosan, etc.

Plant oil triglycerides are the most valuable candidate as a renewable resource due to the wide variety of possibilities for chemical applications and availability all around the world. Hard, though, and load bearing polymeric materials can be produced from plant oil triglycerides. Among them soybean oil is one of the most commonly used plant oils in the world and a group of researchers successfully prepared the load bearing soybean oil based micro composites .[33-34]

On the other hand, the attempts to prepare natural polymeric matrix based nanocomposites are quite limited in the literature. Most of the few studies are concentrated on the renewable polymeric matrixes only [35-41]. These are the works mainly on the synthesis of clay nanocomposites based on renewable plant oils in the presence of

different synthetic intercalants such as alkyl tallow quaternary ammonium salts (like octadecyl ammonium salt and bis(2-hydrpxyethl) ammonium salt) [35, 38-41], (4-vinylbenzyl)triethylammonium chloride which may go to cocrosslinking reaction with the matrix [37]. It was reported that the morphology varies from partially exfoliated to intercalated structure with different types of clay and clay concentrations and mechanical properties are significantly improved by the addition of organoclays. But, in none of these studies, organoclay is modified with a renewable material in order to obtain almost fully renewable polymeric nanocomposites. Therefore, for the purpose of accomplish this aim, in the present study, a polymeric nanocomposite synthesis with both bio based matrix and intercalant was studied.

# 2. AIM OF THE STUDY

The aim of this study is to synthesize renewable polymeric nanocomposites from acrylated epoxidized soybean oil (AESO) by using free radical polymerization technique and to investigate the dynamic mechanical, thermal, and morphological properties of these nanocomposites. This thesis mainly deals with the preparation of renewable polymeric nanocomposites from AESO-S by in-situ polymerization method using a quarternized derivative of functionalized acrylated epoxidized soybean oil (AESO) intercalant which is the first renewable bio-based intercalant in the literature.

To achieve this aim, in the first part of the study:

- Quarternized derivative of functionalized acrylated epoxidized soybean oil (AESO) will be synthesized to use it for modification of montmorillonite (MMT) clay as an intercalant,
- Modification of montmorillonite (MMT) will be done with this bio-based renewable intercalant,

In the second part of the study:

- Synthesis of renewable polymeric nanocomposites will be completed by using modified- montmorillonite (m-MMT).
- Renewable polymeric nanocomposites will be characterized by X-ray diffraction (XRD), atomic force microscopy (AFM), and scanning electron microscopy (SEM) techniques to examine the dispersion states as phase separated, intercalated, or exfoliated.

In the last part of the study,

- The improvements in thermal and dynamic mechanical properties of the resultant nanocomposites and matrix will be evaluated in terms of clay loading and extent of exfoliation by dynamic mechanical analysis (DMA),

differential scanning calorimeter (DSC), and thermogravimetric analysis (TGA).

- Biodegradability properties of the final renewable polymeric nanocomposites and matrix will be investigated by soil burial method.
- In order to confirm biodegradability studies, Lysogeny broth medium will be used, and it will be investigated that if the resultant nanocomposites are antibacterial or not.

# 3. EXPERIMENTAL

Formatted: Normal

## 3.1. Materials

Carbon tetrachloride ($CCl_4$), Tetrahydrofurane (THF), and furfuryl amine (FA) were provided from Merck (Darmstadt, Germany). Styrene (Aldrich-Germany) was used as received. Acrylated Epoxidized soybean oil (AESO) was purchased from The C.P. Hall Company (Chicago, USA) whereas methyl iodide was supplied from Fisher Scientific (New Jersey, USA). Montmorillonite was kindly donated by Süd Chemie (Nanofil 1080, cationic ($Na^+$) exchange capacity of 100 meq / 100 g). 2, 2'-Azoisobutyronitrile (AIBN) was obtained from Merck-Germany and dried in vacuum at room temperature.

## 3.2. Preparation of FA-AESO adduct by Michael Addition of AESO

In order to obtain FA-AESO product, Michael addition reaction was used with reacting furfuryl amine (FA) and acrylated epoxidized soybean oil (AESO). 10,0 g of (0,104 mole) furfuryl amine was dissolved in 50,0 ml THF then the solution of 17,0 g AESO (0,014 mole) in 50,0 ml dry THF was dropped into mixture for 30 min then it was stirred for 5 hours at room temperature . After evaporation of THF, 100,0 ml diethyl ether was added and material was washed with five times with 100 ml water. Ether and all excess furfuryl amine were both evaporated at 40 ºC approximately 6 hours. Details related with the above mentioned reactions are the subject of the study which is a publication of Wool and Küsefoğlu [32]

## 3.3. Quarternization of FA-AESO Adduct

15,0 g of FA-AESO product (0,0097 mole) was dissolved in 50,0 ml dry THF and the solution of 4,86 g $CH_3I$ in 20,0 ml THF was dropped into the FA-AESO solution in 1 hour. Mixture was stirred for 24 hours at room temperature under nitrogen atmosphere. The product was washed with 50 ml of water for five times.

### 3.4. Modification of MMT

Montmorillonite (MMT) clay (1g) was dispersed in 150,0 ml deionized water at 80ºC and a separate solution of quarternized derivative of furfuryl amine functionalized acrylated epoxidized soybean oil (FA-Q-AESO) in 150,0 ml tetrahydrofuran (THF) was heated and mixed at 60ºC for 1hour. FA-Q-AESO solution was then added to the clay solution slowly and mixed vigorously while the temperature of the solution was maintained at 80ºC. After mixing, the total volume is brought up to 300 ml and the solution was stirred for 24hours. The organically modified montmorillonite clay, FA-Q-AESO-MMT, was recovered by filtering the solution followed by repeated washings of the filter cake with deionized water to remove excess ions. The final product was dried at 50 °C in a vacuum oven for 48 hours.

### 3.5. Preparation of Clay Nanocomposites

The desired amount of (1, 2, 3 weight per cent based on the total weight) organically modified montmorillonite clay (FA-Q-AESO-MMT) was added to the monomer mixture which has 50 weight per cent AESO and 50 weight per cent styrene, and was mechanically stirred for 24-72 hours, this pre-mixed mixture was then ultrasonicated for 2-5 hours. With 1 per cent AIBN initiator addition at 45ºC, these mixtures were then cured for 24 hours and post cured at 65ºC for 2 hours, at 85ºC for 2 hours and at 120ºC for 2 hours. To prevent oxygen free-radical inhibition, the resin was purged with nitrogen gas before curing. Formed nanocomposites have been named as AESO-Matrix, AESO-NC1 (1 per cent clay loading), AESO-NC2 (2 per cent clay loading), and AESO-NC3 (3 per cent clay loading).

Table 3.1 shows the nomenclature for renewable polymeric nanocomposites and matrix. Compositions of these nanocomposites can be seen in the Table 3.2

Table 3.1 Nomenclature for nanocomposites

| Polymeric Matrix and Nanocomposites | Amount of Organically Modified MMT (FA-Q-AESO-MMT) (Wt per cent) |
|---|---|
| AESO-M | 0 per cent |
| AESO-NC1 | 1 per cent |
| AESO-NC2 | 2 per cent |
| AESO-NC3 | 3 per cent |

Table 3.2 Composition of the nanocomposite samples

| Polymeric Matrix and Nanocomposites | Styrene (g) | AESO (g) | Organically Modified MMT (g) | Initiator (Wt per cent) |
|---|---|---|---|---|
| AESO-M | 25.0 | 25.0 | 0 | 1.00 |
| AESO-NC1 | 25.0 | 25.0 | 0.505 | 1.00 |
| AESO-NC2 | 25.0 | 25.0 | 1.02 | 1.00 |
| AESO-NC3 | 25.0 | 25.0 | 1.54 | 1.00 |

### 3.6.Characterization

In order to measure the basal spacing (d001 reflection) of montmorillonite (MMT) clays, wide-angle X-ray diffraction (XRD) measurements were conducted on a Rigaku-D/Max-2200 Ultima Diffractometer (Rigaku, Tokyo, Japan) with $CuK_{\alpha}$ radiation ($\lambda$=1,54 Å), operating at 40 kV and 40 mA and a scanning rate of 2º $min^{-1}$. The scanning range is from 1,5º to 10º.

$^{1}H$ NMR (Proton Nuclear Magnetic Resonance) spectra was recorded on a 400 MHz Varian Mercury-VX spectrometer for AESO and FA-Q-AESO samples in d-DMSO.

FTIR (Fourier Transform Infrared) spectra of samples were taken with Perkin Elmer 1600 FTIR spectrometer by using KBr pellets for the AESO and FA-Q-AESO samples.

The dynamic mechanical properties of the nanocomposites were measured with a dynamic mechanical analyzer (DMA Q800, TA Instruments, New Castle, DE, USA) in the single-cantilever mode at a frequency of 1 Hz and a heating rate of 3 °C/min. The samples for the DMA experiments were prepared with a microtome into rectangular shapes having the average dimensions of 12 x 35 x 3 $mm^3$.

Differential scanning calorimetric (DSC) analyses of the nanocomposites were performed with a Differential Scanning Calorimeter (DSC Q200, TA Instruments, New Castle, DE, USA) under a nitrogen atmosphere at a heating rate of 5°C/min.

Thermogravimetric analysis (TGA) was conducted on a TA Instruments TGA-Q50 (New Castle, DE, USA) under a nitrogen flow at a heating rate of 10 K $min^{-1}$ in order to study thermal behavior of the nanocomposite samples.

Atomic Force Microscopy (AFM) was performed using an Universal Scanning Probe Microscope (USPM) (Ambios Technology, Santa Cruz, CA). Phase mode imaging was performed using a silicon nitride cantilever probe with a nominal resonance frequency around 170 kHz and a nominal tip radius of 5-10 nm. Samples were prepared for AFM investigation by first sectioning the molded sample and then mounting it in epoxy potting compound.

Fracture surfaces of the nanocomposites were investigated by using SEM analysis with SEM-FEG & EDAX instrument. SEM images were recorded in the phase mode. E-type scanner was employed with a probing area of 17x17 $mm^2$.

### 3.7. Etching Procedure for AFM Studies

All renewable polymeric nanocomposites and matrix samples were polished by using special sandpapers with 3 μm, 2 μm and 1 μm pore sizes. After sanding procedure, all samples were etched with a special acid solution (4 HCl: 1$HNO_3$: 5 $H_2O$) for a specific time periods. Then, all etched samples were washed with distilled water to remove excess acid from the surfaces of these samples, and all samples were dried by using a drier.

### 3.8. Biodegradability Tests

Biodegradability of the renewable polymeric nanocomposites was studied by using the soil burial method, as described in Goheen and Wool [42]. Nanocomposites and matrix samples were buried in garden soil and the soil was kept moist with deionized water and stored in room at nearly 50 per cent humidity and room temperature. Samples were removed from the soil at regular time intervals of 15 days and washed with distilled water to remove the surface soil. The samples were weighed after drying in the vacuum oven at 50ºC and the weight loss was recorded. The degraded nanocomposites samples' surfaces were studied by using Scanning Electron Microscopy (SEM).

### 3.9. Lysogeny Broth Method

Lysogeny broth (LB), a nutritionally rich medium, is primarily used for the growth of bacteria. It is also known as Luria broth or Luria-Bertani broth. LB media formulations have been an industry standard for the cultivation of *Escherichia coli* as far back as the 1950s. These media have been widely used in molecular microbiology applications for the preparation of plasmid DNA and recombinant proteins. It continues to be one of the most common media used for maintaining and cultivating recombinant strains of *Escherichia coli*. [43]


Figure 3.1 LB Medium Bottle and LB Agar Plate

There are several common formulations of LB. Although they are different, they generally share a somewhat similar composition of ingredients used to promote growth of bacteria. This method is used in this study in order to investigate that these nanocomposites have not antibacterial properties and to confirm the results of the previous biodegradability studies. All samples were installed into the LB agar plate for two weeks, and then nanocomposites samples' surfaces were studied by using Scanning Electron Microscopy (SEM) and optical microscopy methods. Promotion of the growth of bacteria on nanocomposites and matrix's surface was followed.

# 4. RESULTS AND DISCUSSION

## 4.1. Synthesis and Characterization of Quarternary Derivative of AESO

The most important point of this thesis study is to synthesize renewable bio-based intercalant for the purpose of modifying montmorillonite (MMT) clay, because this intercalant must be suitable for synthesizing renewable polymeric nanocomposites. In order to obtain totally renewable polymeric nanocomposites, it is very important to obtain suitable intercalant from renewable resources. It is believed that the usage of AESO-based intercalant is very important for AESO-based nanocomposites synthesis due to well-known compatibility which may lead to exfoliation structure.

Firstly, by using necessary reactants, FA-AESO (furfuryl amine functionalized derivative of acrylated epoxidized soybean oil) was synthesized from AESO. Acrylate double bonds of acrylated epoxidized soybean oil (AESO) are very susceptible towards nucleophilic attack which makes them good Michael acceptors. FA-AESO adduct can be easily synthesized by reacting acrylated epoxidized soybean oil (AESO) with furfuryl amine (FA) via Michael addition reaction. All reaction steps can be seen in Figure 4.1. The reaction was carried by mixing the reactants in a certain ratio. In order to prove the success of this synthesis $^{1}$H NMR and FTIR spectroscopic methods were used.

$^{1}$H NMR analysis of acrylated epoxidized soybean oil (AESO) and furfuryl amine functionalized derivative of acrylated epoxidized soybean oil (FA-AESO) were done by using Nuclear Magnetic Resonance (NMR) spectroscopy technique.

Figure 4.2 shows the $^{1}$H NMR spectrums of AESO and FA-AESO. The characteristic peaks of AESO (Figure 4.2 a) are peak 1 appearing at 0.8 ppm which corresponds to methyl protons of the fatty acid chains; peak 2 appearing at 2.2ppm which corresponds to protons of $\alpha$ to the carbonyl; peak 3 appearing in the 4.0 - 4.4 ppm range, corresponds to –$CH_2$ protons of the glycerol unit; peak 4 appearing at 5.2 ppm, which corresponds to –CH- proton of the glycerol unit; and peak 5, 6, and 7 appearing at 5.8, 6.0, and 6.3 ppm, corresponds to –CH=$CH_2$ protons of the acrylate esters.

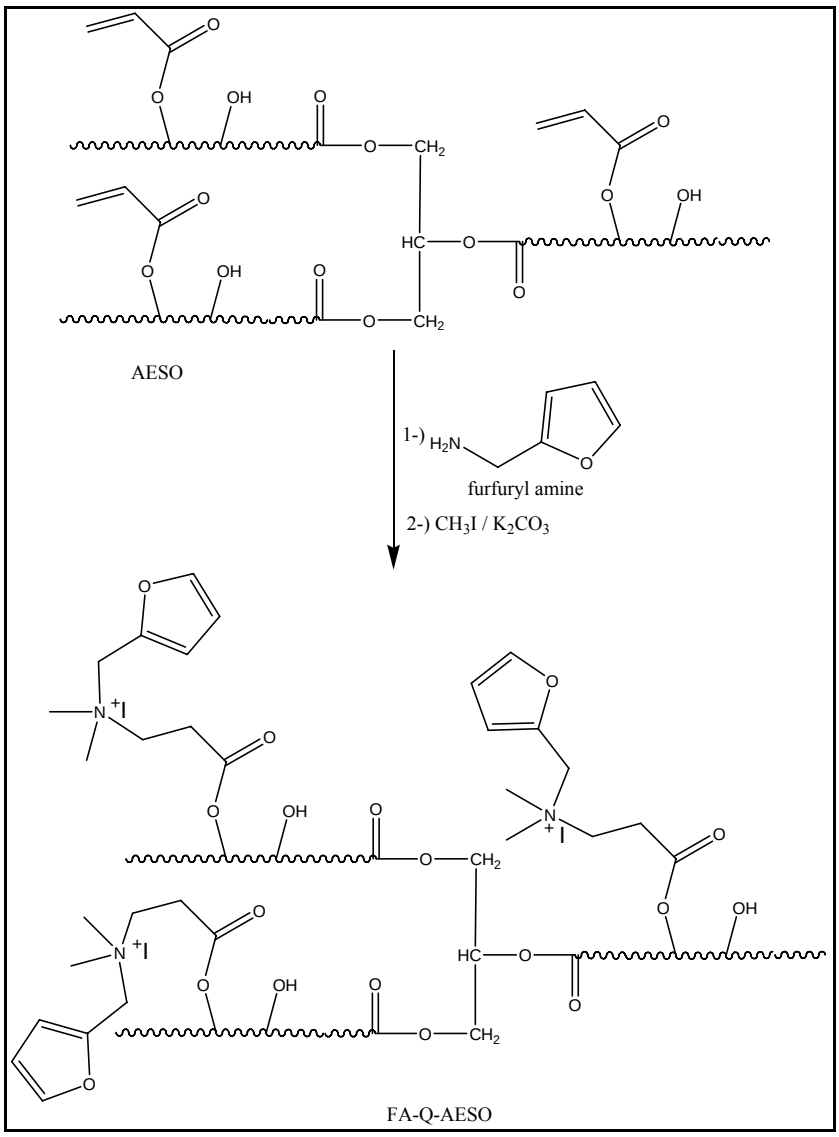


Figure 4.1 Preparation and quarternization of FA-AESO adduct

In the NMR spectrum of the FA-Q-AESO (Figure 4.2 b), there are some differences from the NMR spectrum of AESO. In this spectrum, all characteristic peaks related with –$CH{=}CH_2$ groups disappeared (peaks at 5.8, 6.0, and 6.3 ppm) which means that the reaction with reaction with double bonds of acrylate groups and furfuryl amine is successful. There are new peaks appearing at 7.2 ppm which corresponds to furane ring's protons. The other peaks at 1.8, 3.6, and 7.5 ppm corresponds to –N-aryl groups' protons,

these peaks prove that the reaction between furfuryl amine and AESO is successful and at the end of the reaction quarternized derivative of functionalized AESO ) (FA-Q-AESO) was formed.

In the FTIR spectrum of AESO (I) and FA-Q-AESO (II):

I) FTIR υ ($cm^{-1}$): 3434 (br, O-H), 2928 (s, -$CH_2$-), 2856 (s, C-H), 1726 (s, C=O), 1635 (m, C=C), 1608 (m, C=C), 1509 (m,-C-H), 1295 (s, -CH-OH, Def.), 1196 (s, C=O), 985 (s, C=C), 810 (m, =$CH_2$, twisting), 782 (s, -$CH_2$-, skeleton-rocking), 638 (m, -C-H, out of plane)

II) FTIR υ ($cm^{-1}$): 3377 (br, O-H), 3104 (s, C-H), 2919, (s, C-H), 2848 (m, O-C-H), 1732 (s, C=O), 1607 (s, C=C), 1498 (w, C-NH-C), 1462 (m, -$CH_2$-), 1376 (s, -O-CO-$CH_2$), 1183 (w, C-N stretching), 1072 (s, -C-O-H), 1014 (s, aromatic ring C-H, Def.), 1008 (s, aromatic ring C-H, Def.), 752 (m, -$CH_2$-, Def.), 599 (m, furane ring Def.)

In the FTIR spectrum of AESO (Figure 4.3 b), it can be easily seen that there are some peaks corresponding to acrylate groups such as 1635, 985, 810,638; and these peaks disappeared in the FTIR spectrum of FA-Q-AESO. Peak at 1635 $cm^{-1}$ corresponds to acrylate double bonds which are near to the carbonyl group. Peak at 985 $cm^{-1}$ also corresponds to deformation vibration of acrylate groups. Peak at 810 $cm^{-1}$ corresponds to twisting vibration of =$CH_2$ group of acrylate group.

In the FTIR spectrum of FA-Q-AESO (Figure 4.3 c), there are some different peaks which prove the furfuryl amine linkage to the acrylate group of AESO. These peaks are at 1183 $cm^{-1}$ corresponds to C-N stretching vibration, 1014 $cm^{-1}$ and 1008 $cm^{-1}$ peaks correspond to aromatic furane ring C-H deformation vibration. Peak at 3104 $cm^{-1}$ corresponds to C-H stretching vibration of C=C-H due to aromaticy of furane ring.

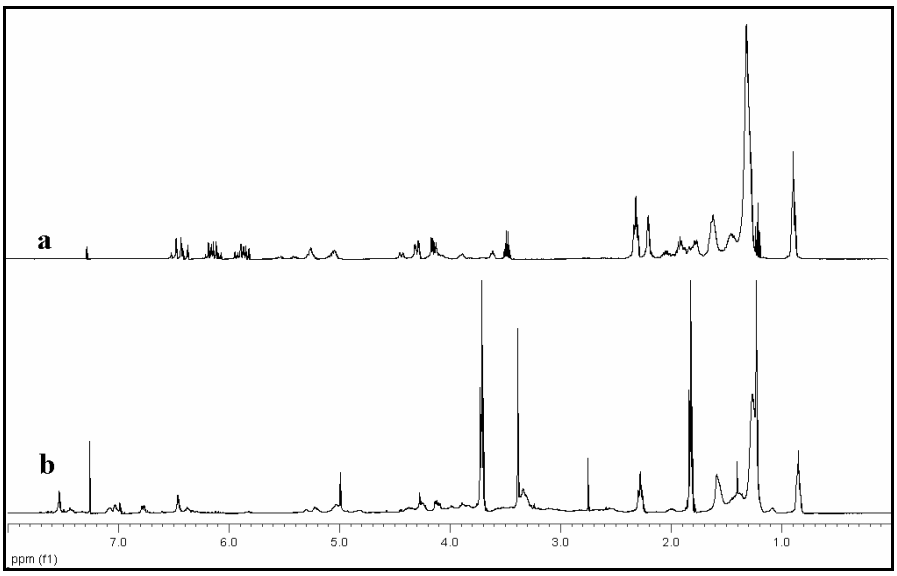


Figure 4.2 $^{1}$H NMR spectra of a) AESO, b) FA-AESO

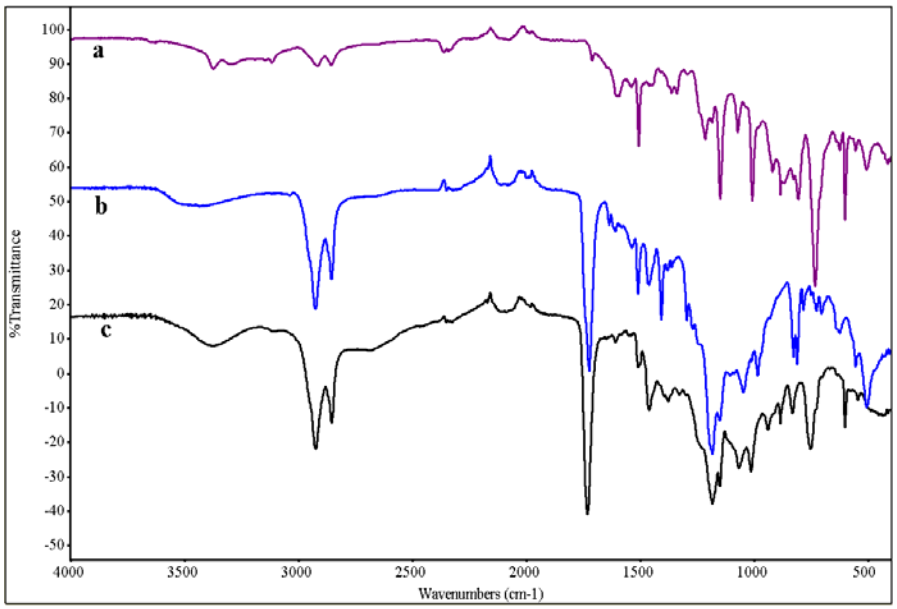


Figure 4.3 FTIR Spectra of a) Furfuryl Amine, b) AESO, and c) FA-AESO

### 4.2.Modification of MMT

In this part of the study, new renewable bio-based quarternized derivative of AESO (FA-Q-AESO) was studied as intercalant; it was used in order to modify montmorillonite (MMT) clay.

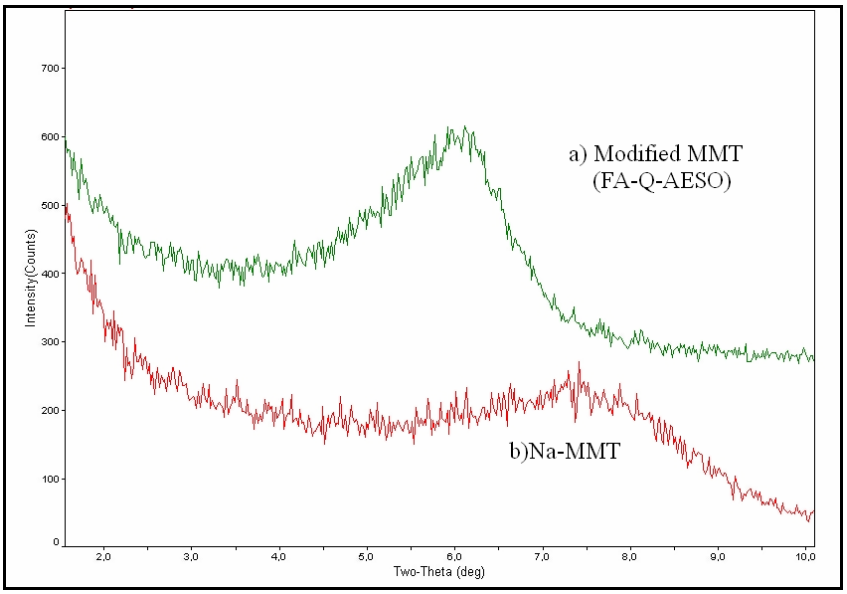


Figure 4.4 XRD analysis of Na-MMT and modified-MMT (FA-Q-AESO-MMT)

Modification of the montmorillonite (MMT) clay was followed with X-ray diffraction (XRD) analysis. The diffraction patterns were monitored between 1,5º and 10º with a scanning rate of 2º/min. Basal spacing of montmorillonite (MMT) and modified-MMT were obtained from the peak position of the door reflections in the XRD patterns.

Figure 4.4 shows the XRD analysis of Na-MMT and modified-MMT (FA-Q-AESO-MMT), there is an increase in interlayer spacing indicating an ordered intercalated system with the FA-Q-AESO modifier, so this new renewable bio-based quarternized derivative of soybean oil works as an intercalant successfully. Basal spacing (or d-spacing) was found to be 12.05 Aº for Na-MMT (Figure 4.4 b). After modification, basal spacing increased to 14.95 Aº indicating that the intercalation of the quarternized derivative of acrylated

epoxidized soybean oil (AESO) into the montmorillonite (MMT) was successful resulting in an organophilic clay (Figure 4.4 a).

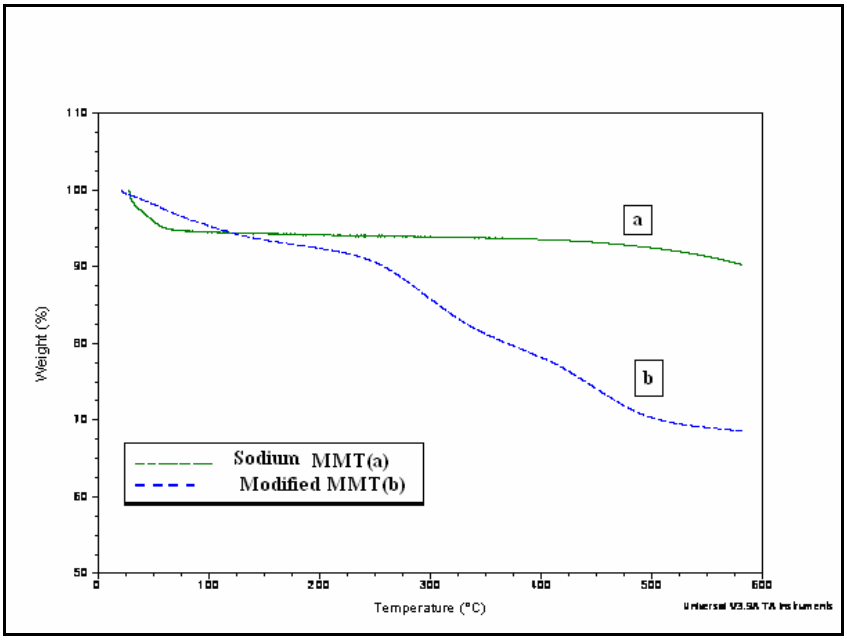


Figure 4.5 TGA Thermograms of a) Sodium MMT and b) Modified MMT

Thermogravimetric analysis (TGA) is used to prove the intercalation of FA-Q-AESO into interlayer galleries as well as to obtain the thermal stability data of sodium montmorillonite, and modified montmorillonite (FA-Q-AESO-MMT)

Figure 4.5 shows TGA thermograms of sodium montmorillonite (MMT) clay (a) and modified montmorillonite clay (FA-Q-AESO-MMT) (b). In the thermograms, it can be easily seen that, there is a big difference in their degradation amounts which is directly related with the amounts of organic material which natural or modified MMT has in its structure. The degradation amount of natural montmorillonite (MMT) is 9.74 weight per cent, but it is 31.20 weight per cent for modified montmorillonite (FA-Q-AESO-MMT). As it can be seen from these thermograms,organic part of the clay was increased by using functionalized quarternized derivative of AESO (FA-Q-AESO), modification of montmorillonite (MMT) was successfully achieved.

### 4.3. Synthesis and Characterization of the Nanocomposites

Schematic representation of the synthesis of AESO-based nanocomposites can be seen in Figure 4.6.

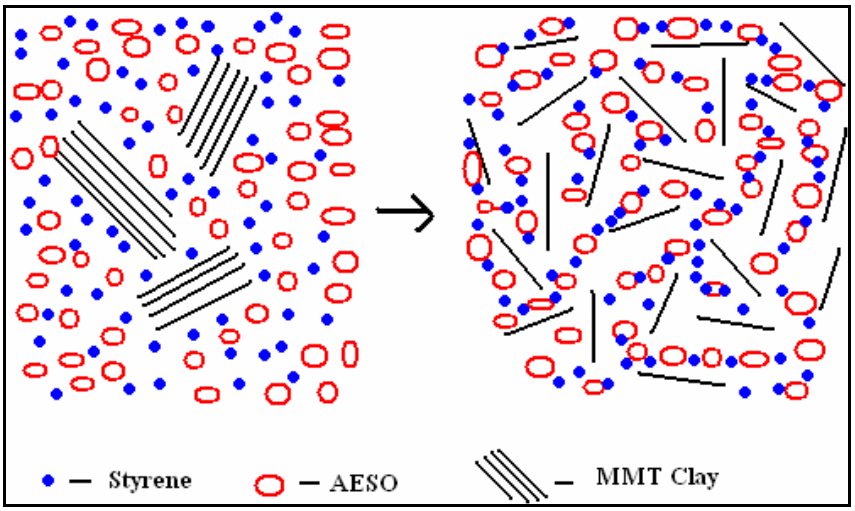


Figure 4.6 Schematic representation of the synthesis of the nanocomposites

After the completion of the modification of montmorillonite (MMT) clay with FA-Q-AESO intercalant, modified montmorillonite (FA-Q-AESO-MMT) was obtained, by using this compatible modified clay and AESO-S monomer solution, nanocomposites with different clay loadings were prepared. In order to synthesize these nanocomposites, in-situ free radical polymerization technique was used. All nanocomposites were firstly characterized with XRD (X-Ray Diffraction) to investigate structural properties of the nanocomposites. Then, all mechanical and thermal properties were found by using DMA, DSC, and TGA analysis methods. Finally, AFM and SEM methods were used to have information about the morphological properties of the nanocomposites.

### 4.3.1. Structural Properties of the Nanocomposites

XRD analysis was used to identify nanocomposite structures with the calculation of the basal reflections of the separated silicate layers by monitoring the position, shape and intensity of these reflections.

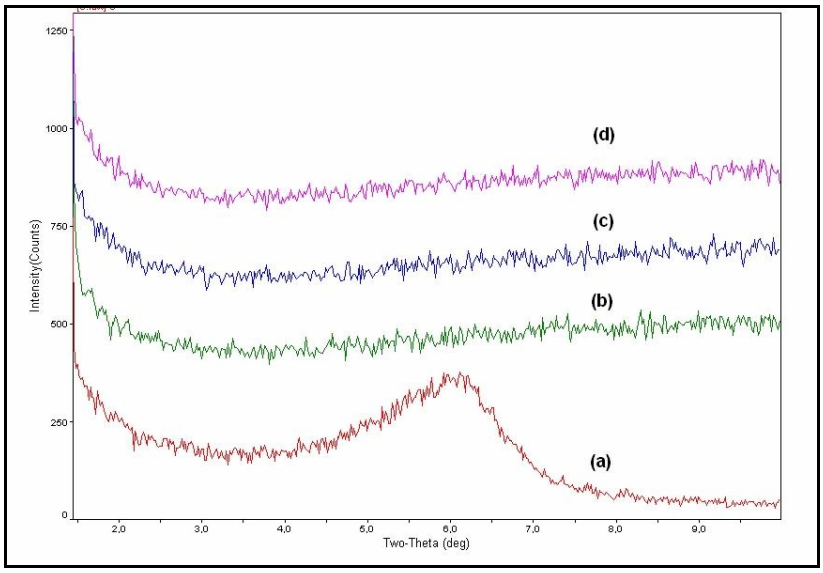


Figure 4.7 XRD traces of modified-MMT (a), AESO-NC1 (b), AESO-NC2 (c), and AESO-NC3 (d)

Figure 4.7 shows the XRD curves of modified montmorillonite (FA-Q-AESO-MMT) and nanocomposites. The absence of any peak in the diffractograms of all nanocomposite compositions (Figure 4.7) indicates that the layer structure of the clays has been broken down and the clay platelets are well separated from each other, so the clays are exfoliated. In all nanocomposite compositions, exfoliation structures were obtained.

### 4.3.2. Mechanical Properties of the Nanocomposites

The dynamic mechanical performance of acrylated epoxidized soybean oil (AESO) matrix and its nanocomposites are investigated via dynamic mechanical analyzer (DMA). Two different dynamic mechanical parameters were determined as a function of

temperature. It is very well known that the storage modulus represents the elastic component response related to the potential energy stored in the viscoelastic material under deformation and is a measure of rigidity. On the other hand, the loss factor (tan delta) is one of the damping parameters of interest since it is a measure of ability of the polymer to convert mechanical energy into heat at a temperature or frequency of interest. The temperature of tan delta peak also corresponds to the glass transition temperature of the material. At the glass transition temperature, a polymer is more efficient in converting sound and mechanical vibration energy into heat, which results in absorption. A shift in the position of the tan delta peak to higher temperatures would thus indicate improved thermo mechanical properties at those conditions.

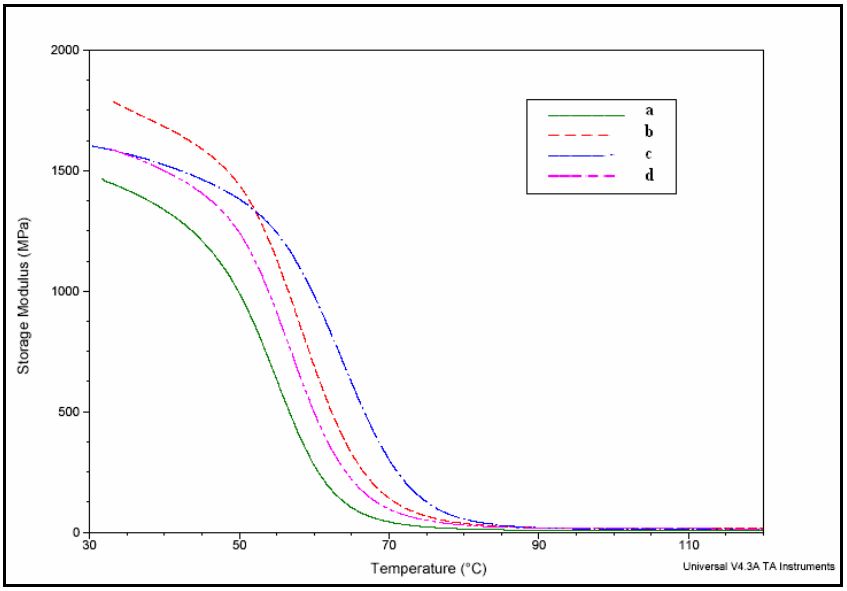


Figure 4.8 Storage modulus versus temperature plots of the AESO matrix (a) AESO-NC1 (b), AESO-NC2 (c) and AESO-NC3 (d) samples

The temperature dependence of storage modulus and of tan delta for virgin acrylated epoxidized soybean oil (AESO) polymer and its nanocomposites are shown in Figure 4.8 and Figure 4.9.

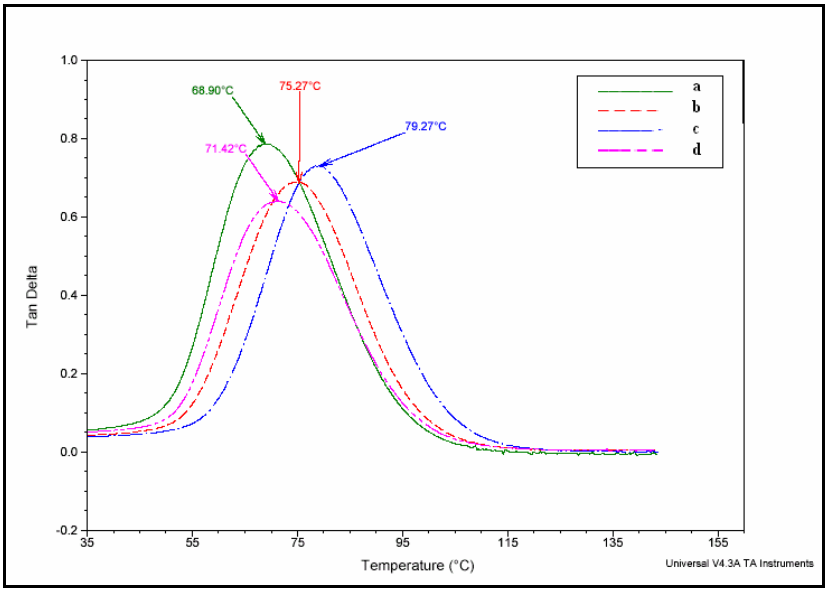


Figure 4.9 Tan delta versus temperature plots of the AESO matrix (a) AESO-NC1 (b), AESO-NC2 (c) and AESO-NC3 (d) samples.

The moduli of the all nanocomposites as well as tan delta peak temperatures are observed to be higher than that of the neat acrylated epoxidized soybean oil (AESO) matrix. Both shift and broadening of tan delta peak towards higher temperatures and increase in storage modulus values for the nanocomposites may be ascribed to their exfoliation morphologies with fine dispersion of organoclay layers in the polymer matrix leading to that provided a large aspect ratio for the clay, This increased polymer-clay interactions, making the entire surface area of the clay layers available for the polymer causing to restricted segmental motions near organic-inorganic interfaces [44] and therefore leading to dramatic changes in the mechanical properties [45]. The 3 % loaded nanocomposite exhibiting relatively weak thermal stability and low glass transition temperature, on the other hand, appears to have also lower storage modulus and tan delta peak temperature than the other nanocomposites most probably due to the decrease in rigidity by loss of styrene outside the clay layers as also reported by other authors [46-47].

Compared to virgin AESO-based polymer, all the nanocomposites obtained were found to have higher tan delta peak temperatures. The shift and broadening of the tan delta

peak to higher temperatures indicate an increase in glass transition temperatures (Tg) and enhanced thermomechanical properties. Tan delta peak temperatures of the nanocomposites increases (Figure 4.9) in a good agreement with the increase in storage modulus values (Figure 4.8).

Table 4.1 summarizes the dynamic mechanical properties of renewable polymeric nanocomposites and matrix. Storage moduli values (E') and glass transition temperatures for these nanocomposites and matrix can be seen in this table.

Figure 4.9 shows that all the nanocomposites have higher stiffness than the virgin AESO-M polymer as evidenced by lower tan $\delta_{max}$ values. This can be attributed to good dispersion of modified- montmorillonite (FA-Q-AESO-MMT) layers in AESO-M polymer matrix leading to a large surface area of the clay interacting with the polymer preventing the segmental motions of the polymer chains.

It is known that the presence of organoclay in nanocomposites generally improves the stiffness of materials leading to a higher storage modulus. But, it is also possible that organoclays may serve as a plasticizer in the nanocomposite, resulting in a decrease in storage modulus.

Therefore, decrease in storage modulus and tan delta peak temperature for the AESO-NC-3 nanocomposite may be attributed to the plasticizing effect of organically modified- montmorillonite (FA-Q-AESO-MMT) clay in AESO-M matrix. It can be said that with an increase in the nanofiller content of the nanocomposites, plasticizing effect increases.

Table 4.1 Dynamic Mechanical Properties of Renewable Nanocomposites

| Polymer Matrix and Nanocomposites | Organoclay Content (Wt per cent) | Storage Modulus (MPa) at 35 ºC | Tg (ºC) |
|---|---|---|---|
| AESO-M | 0 | 1464 | 69,5 |
| AESO-NC1 | 1 | 1786 | 75,2 |
| AESO-NC2 | 2 | 1602 | 79,2 |
| AESO-NC3 | 3 | 1592 | 72,1 |

Table 4.2 Dynamic Storage Moduli of the AESO-based clay nanocomposites at various temperatures

| Polymer Matrix and Nanocomposites | Organoclay Content (Wt per cent) | Storage Modulus (MPa) at different temperatures | | |
|---|---|---|---|---|
| | | 25ºC | 50 ºC | 100 ºC |
| AESO-M | 0 | 1464 | 992 | 6,6 |
| AESO-C1 | 1 | 1786 | 1461 | 15,11 |
| AESO-NC2 | 2 | 1602 | 1398 | 11,55 |
| AESO-NC3 | 3 | 1592 | 1243 | 14,10 |

Some values of storage moduli at various temperatures are presented in Table 4.2. AESO-NC1 has the highest storage modulus values for all temperatures. As the temperature increases, matrix shows lower storage modulus compared to nanocomposites. Actually as the temperature increases, the storage moduli of all samples exhibit drop, but matrix sample drops sharply. Then all of the nanocomposite samples and matrix show modulus plateau after temperature 70 ºC. Apparently, the modulus drop corresponds to onset of segment mobility in the crosslinked polymer networks. These results show clearly that the addition of modified montmorillonite (m-MMT) clay into AESO-M matrix results in a remarkable increase of stiffness.

### 4.3.3. Thermal Properties of the Nanocomposites

Thermogravimetric analysis (TGA) is used in order to obtain the thermal stability data of the renewable polymeric nanocomposites and matrix.

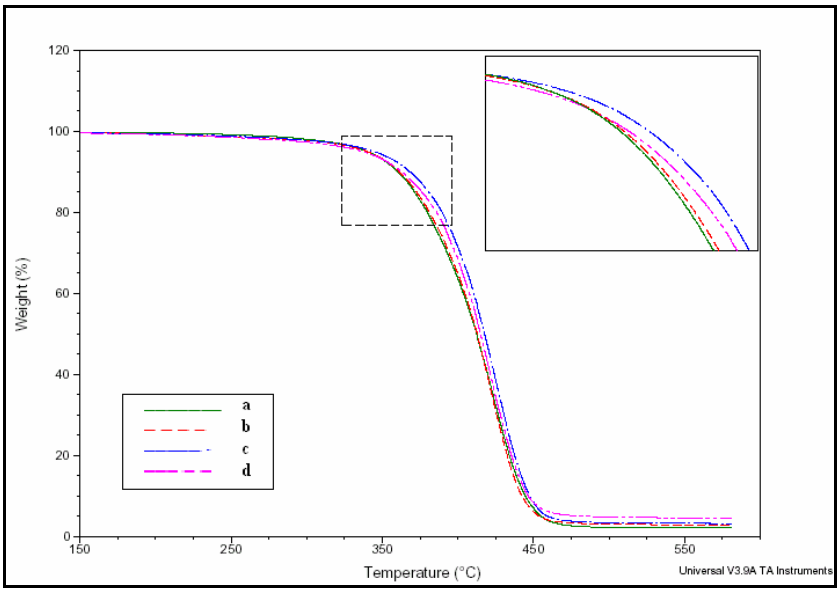


Figure 4.10 TGA Thermograms of the AESO matrix (a), AESO-NC1 (b), AESO-NC2 (c), and AESO-NC3 (d) samples

Figure 4.10 shows TGA thermograms of virgin acrylated epoxidized soybean oil (AESO) polymer and its nanocomposites with different nanofiller loadings. As compared with matrix, the resulting nanocomposites were found to have significant improvements both in thermal and flame resistance properties with higher degradation onset temperatures and high char content.

The onset degradation temperatures of all nanocomposites are higher than virgin matrix; moreover improvement reaches to almost 15 °C with only 2 % loading. The origin of this increase in the decomposition temperatures mainly results from the dispersed nanoscale silicate layers hindering the permeability of the volatile degradation products out of the material [47] resulting also in high char yields. On the other hand , a slight

decrease in degradation temperature for 3 % loading may be attributed to either possible existence of small amount of clay tactoids , although microstructure analyses does not confirm such tactoid formations or loss of styrene outside the clay as observed by several authors [48].

Table 4.3 TGA Data for AESO Nanocomposites and Matrix

| Polymer Matrix and Nanocomposites | $Td_{10}$ (°C) | $Td_{50}$ (°C) | Char (per cent) at 600 °C |
|---|---|---|---|
| AESO-M | 353,45 | 410,29 | 2,091 |
| AESO-NC1 | 361,45 | 413,71 | 2,769 |
| AESO-NC2 | 368,30 | 417,67 | 3,125 |
| AESO-NC3 | 362,97 | 414,95 | 4,427 |

Table 4.3 and Table 4.4 summarizes the TGA data of the acrylated epoxidized soybean oil (AESO) based nanocomposites and matrix. All nanocomposites exhibited enhanced thermal stabilities compared to virgin AESO-based polymer. The temperature at which 10 per cent degradation occurs ($Td_{10}$) as representative of the onset temperature of degradation which was found to be increased. The mid-point degradation temperature ($Td_{50}$) was also found to be higher for the renewable polymeric nanocomposites than virgin AESO-based polymer. According to TGA data, it can be said that 2 per cent loaded nanocomposite (AESO-NC-2) seems to have the highest thermal stability relative to other nanocomposite compositions.

Table 4.4 TGA Results of Weight Loss for AESO Nanocomposites

| Polymer Matrix and Nanocomposites | Weight Loss ( wt per cent) | | | |
|---|---|---|---|---|
| | 0-300 °C | 300-400 °C | 400-500 °C | 500-600 °C |
| AESO-M | ~2 | ~35 | ~95 | 98 |
| AESO-NC1 | ~2 | ~35 | ~95 | 97,3 |
| AESO-NC2 | ~2 | ~35 | ~95 | 96,9 |
| AESO-NC3 | ~2 | ~35 | ~95 | 95,5 |

Table 4.4 shows the characteristic temperatures in TGA curves (Figure 4.10), it can be easily seen that AESO-based renewable polymeric nanocomposites appear to be thermally stable at temperatures up to 350 ºC. These materials lose about 35 per cent of their weight at the temperature between 300 and 400 ºC; there is an abrupt weight loss after nearly 350 ºC. A 95 per cent weight loss was observed at 500 ºC. There is no significant difference between matrix and nanocomposite samples with different clay loading under $N_2$ atmosphere at 500 ºC. But, at the final stage, there were some differences due to the different char content of these samples.

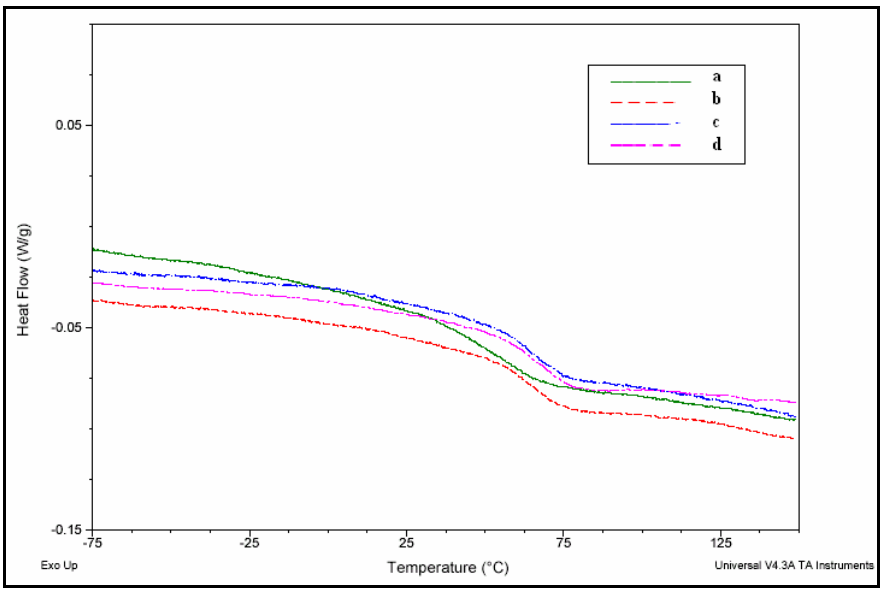


Figure 4.11 DSC Thermograms of the AESO matrix (a) AESO-NC1 (b), AESO-NC2 (c), and AESO-NC3 (d) samples

The thermograms related with thermal transitions of pure matrix and nanocomposites studied with differential scanning calorimeter (DSC) are all given in Figure 4.10.

The effect of dispersed individual clay platelets on glass transition temperature (Tg) of matrix can be easily seen with the shift to higher temperatures indicating restricted segmental motions of polymer chains at the organic-inorganic interface due to the confinement of acrylated epoxidized soybean oil (AESO) polymer chains between the

silicate layers as well as silicate surface- polymer interaction in nanostructure hybrids. On the other hand, slight decrease in also the Tg values of the 3 % loaded nanocomposite is obvious in the thermogram. It can be attributed to the possible plasticizing effect of the styrene lost from the interlayer galleries which causes to low thermal stabilities confirmed by the previous thermo gravimetric (TGA) analysis.

### 4.3.4. Morphological Properties of the Nanocomposites

The extent of clay dispersion in the nanocomposites was also studied with atomic force microscopy (AFM). Figure 4.12 shows high magnification AFM images of nanocomposites in phase mode. The phase images of the filled nanocomposites revealed the presence of clay plates as the bright features in the dark polymer matrix. A nanoscale dispersion of individual clay layers can be clearly observed in all loading degrees confirming the exfoliation structure as a good agreement with the facts shown in XRD patterns.

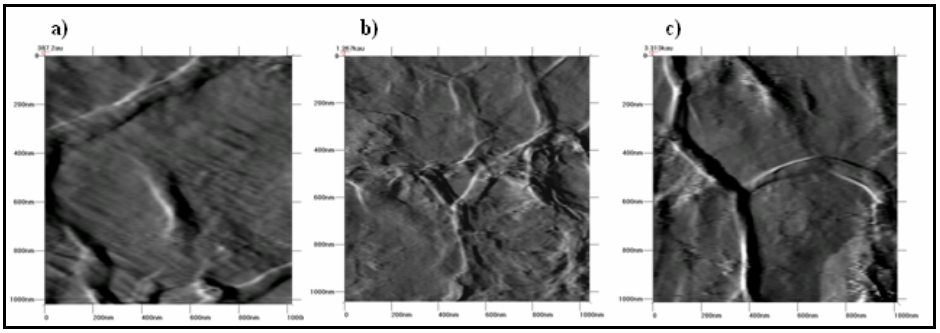


Figure 4.12 High magnification AFM images of AESO-NC1 (a), AESO-NC2 (b), and AESO-NC3(c).

Fracture surfaces of AESO-based matrix and its renewable bio-based polymeric nanocomposites were studied with Scanning Electron Microscopy (SEM) in order to obtain morphological features of these polymeric materials.

Figure 4.13– 4.15 show low magnification scanning electron (SEM) micrographs of the fracture surfaces of AESO-based matrix and its nanocomposites containing 1, 2, and 3

weight per cent organically modified montmorillonite clay (FA-Q-AESO-MMT). All fracture surfaces were extremely flat. These suggest that the behavior of the AESO-based matrix and its nanocomposites were plastic. The phase separation was not observed in all nanocomposites and matrix. Therefore, it can be said that acrylated epoxidized soybean oil (AESO), styrene, and organically modified montmorillonite (FA-Q-AESO-MMT) were homogeneously mixed and then cured.

In the micrographs of the nanocomposites, it can be easily seen that nanocomposites have very smooth surfaces. It is evident from the micrographs that the morphology of the nanocomposites has a homogeneously dispersed phase of organoclays within the acrylated epoxidized soybean oil (AESO) matrix. This is in accordance with the X-ray diffraction (XRD) results discussed earlier (Figure 4.7).

AESO-based renewable polymeric nanocomposites have smooth surfaces with relatively small clay particles that are more homogeneously dispersed in the AESO-BASED matrix. This morphology for these nanocomposites can be attributed to the effective in-situ polymerization from both interlayer galleries and surfaces/edges which then resulting in well dispersion of silica layers in the form of exfoliated structure which also confirmed by XRD analysis.

The good dispersion of organically modified montmorillonite clay (FA-Q-AESO-MMT) in the matrix is well consistent with the XRD data without any $d_{001}$ reflection (Figure 4.7) and the high stiffness, glass transition temperature and damping temperature for the AESO-based renewable polymeric nanocomposites. So, the scanning electron microscopy (SEM) analysis confirmed the results of X-ray diffraction (XRD) analysis for these renewable polymeric nanocomposites.

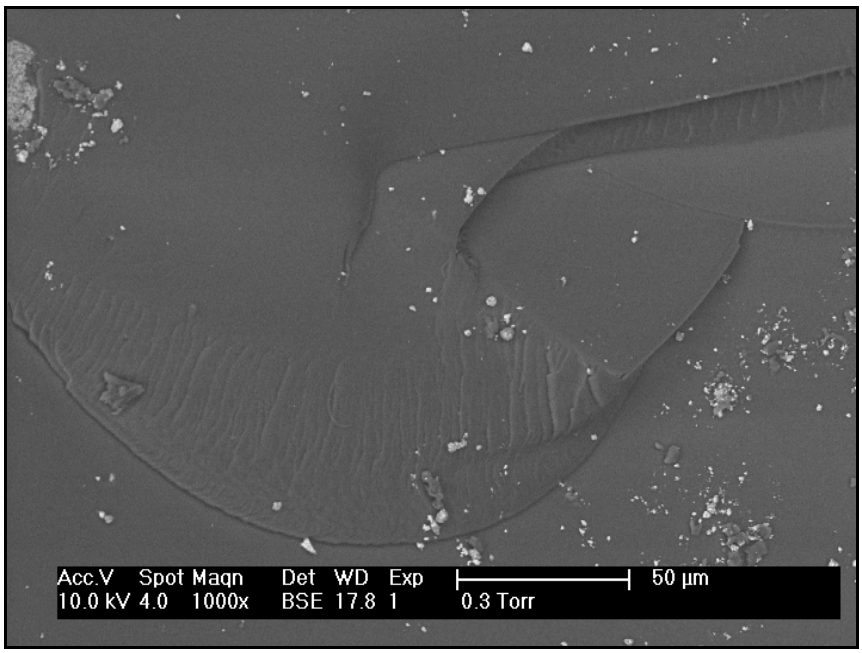


Figure 4.13 Low magnification SEM micrograph of AESO-NC1

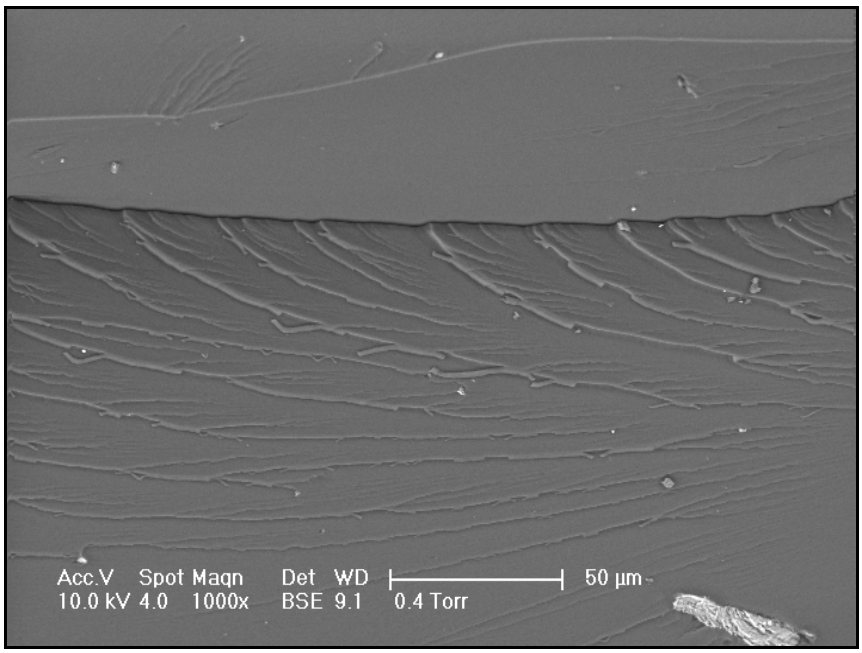


Figure 4.14 Low magnification SEM micrograph of AESO-NC2.

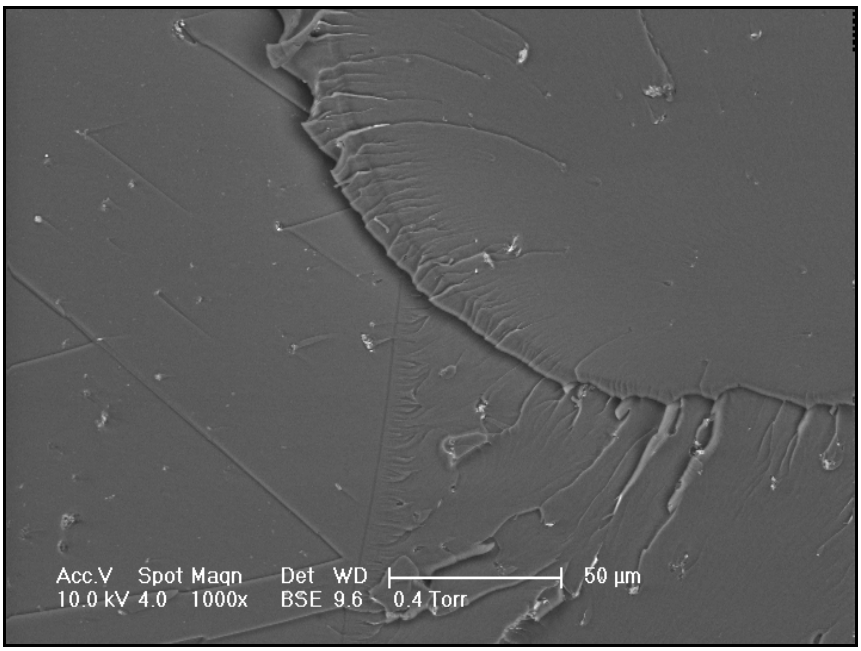


Figure 4.15 Low magnification SEM micrograph of AESO-NC3.

Figure 4.16 – 4.18 show high magnification SEM micrographs of the fracture surfaces of AESO-based matrix and its nanocomposites containing 1, 2, and 3 weight per cent organically modified MMT clay (FA-Q-AESO-MMT). High magnification scanning electron microscopy (SEM) images of nanocomposites exhibited again homogeneous fracture surfaces with a crack propagation along a tortuous path and may be ascribed to good dispersion of organically modified montmorillonite clay (FA-Q-AESO-MMT) in the matrix.

In the SEM micrographs of nanocomposites, the river lines (shear steps) on the fracture surfaces of the nanocomposites indicate high toughness. (Figure 4.16 – 4.18)

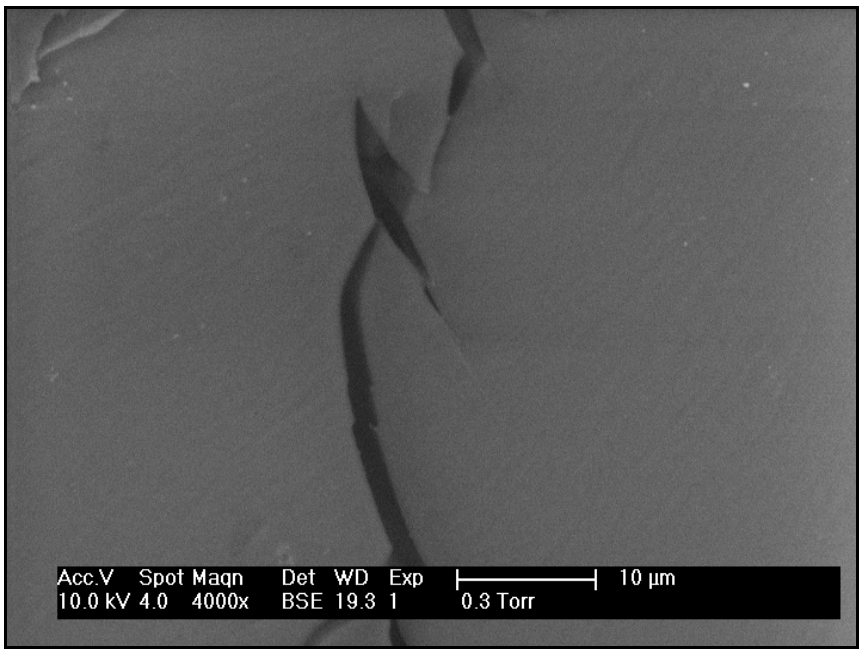


Figure 4.16 High magnification SEM micrograph of AESO-NC1

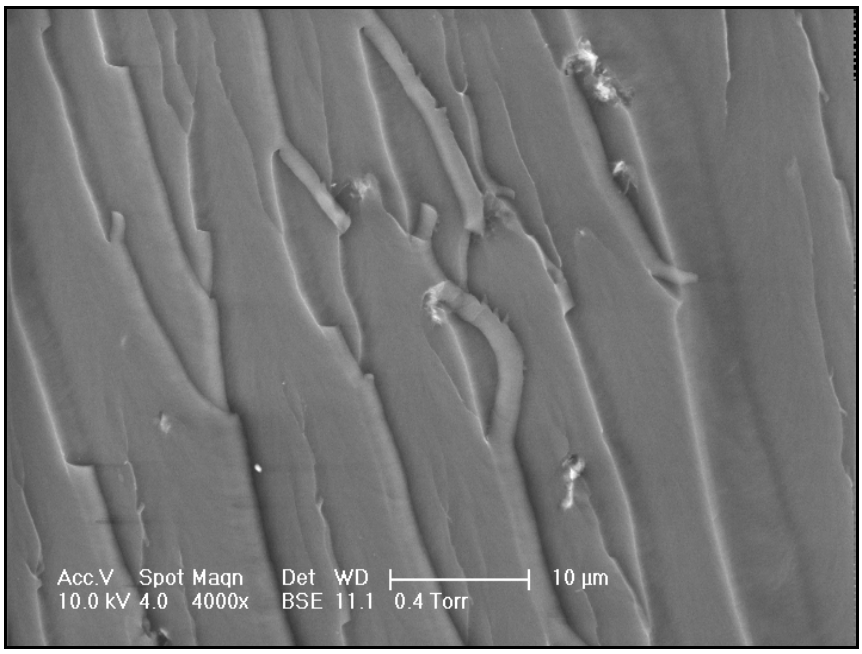


Figure 4.17 High magnification SEM micrograph of AESO-NC2

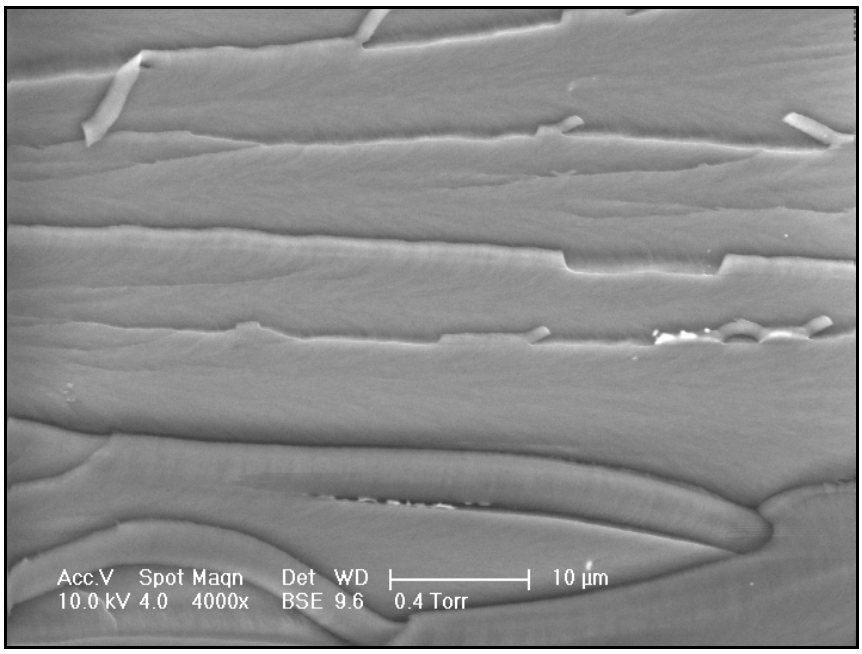


Figure 4.18 High magnification SEM micrograph of AESO-NC3

Atomic force microscopy (AFM) studies were conducted on polished, physically ablated ("etched" by acid mixture) surfaces of the nanocomposites specimens, the atomic force microscopy (AFM) operated in tapping mode and the amplitude- and height-contrast images were captured.

The AFM phase images of the renewable bio based polymeric nanocomposites with different organically modified montmorillonite clay (FA-Q-AESO-MMT) loading are illustrated in Figure 4.19 - 4.120. Some distinct white bright features are observed, which are representing clay platelets. Similar observation is made when a large number of areas were analyzed at different magnifications.

In low and high magnification atomic force microscopy (AFM) pictures, it can be seen that the organically modified montmorillonite clay (FA-Q-AESO-MMT) is delaminated (or exfoliated) in the AESO-based polymer matrix. In these nanocomposites, acrylated epoxidized soybean oil (AESO) is soft and can be more easily ablated than the styrene during etching procedure with acid mixture. Therefore, the formation of an AESO-

rich interphase is well documented in these AFM figures. It can be concluded that organically modified montmorillonite clay (FA-Q-AESO-MMT) (which is modified with oil based intercalant) can more easily exfoliated in these oil based nanocomposites.

Figure 4.19 and Figure 4.20 show the tapping mode atomic force microscopy (AFM) phase images at a scan size of 1μm and 2 μm for the nanocomposites. Excellent contrast exists between the clay platelets and the polymer matrix. As it can be seen from the images, all nanocomposites have small clay particles and very good distribution in polymer matrix which is in good agreement with X -ray diffraction (XRD) and scanning electron microscopy (SEM) data.

The phase images of the filled nanocomposites revealed the presence of organically modified montmorillonite clay (FA-Q-AESO-MMT) nanofillers as the bright features in the dark polymeric matrix. These features are also observed in the 3D-phase images of the nanocomposites. (Figure 4.21)

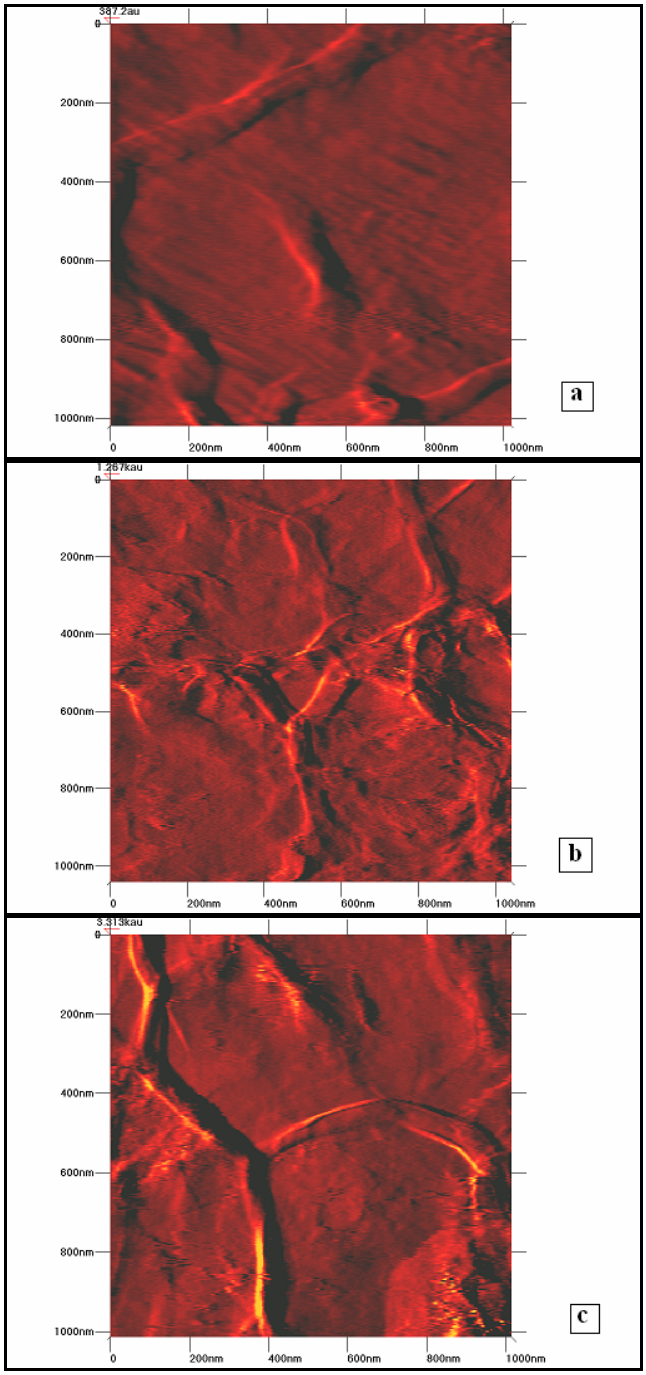


Figure 4.19 High magnification AFM images of a) AESO-NC1,b) AESO-NC2, and c) AESO-NC3.

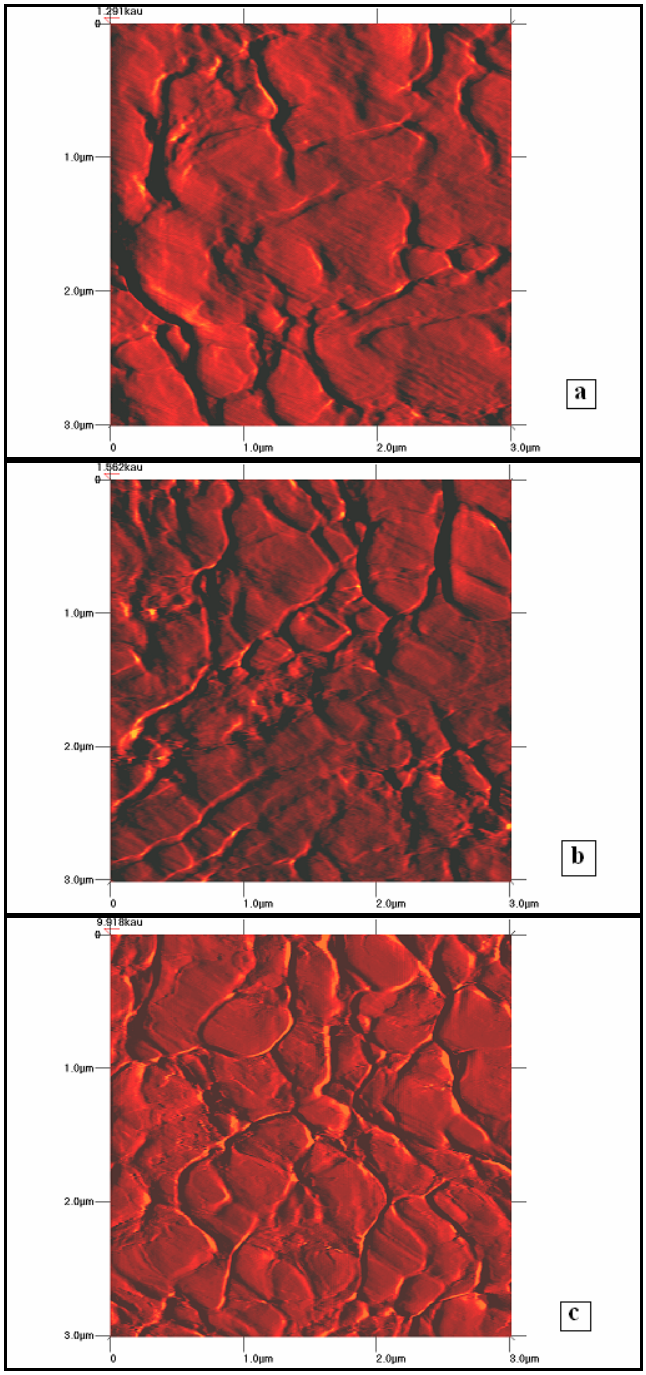


Figure 4.20 Low magnification AFM images of a) AESO-NC1,b) AESO-NC2, and c) AESO-NC3.

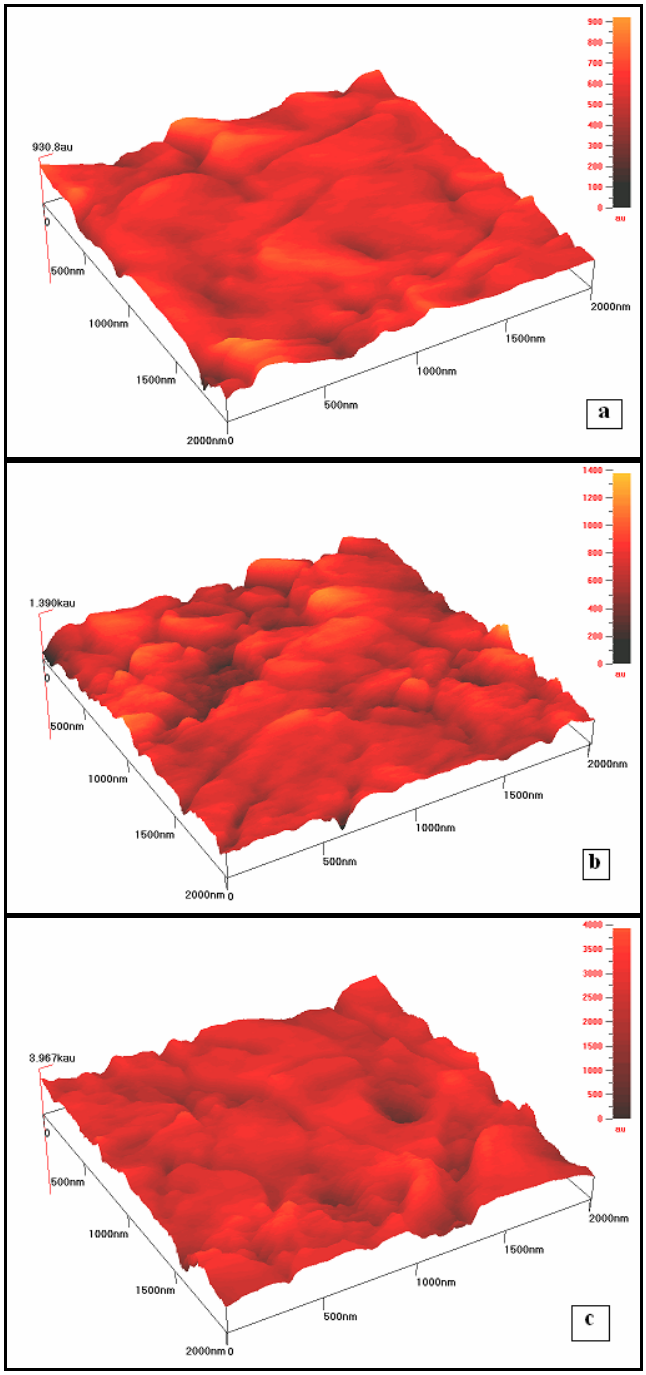


Figure 4.21 a) AESO-NC1, b) AESO-NC2, and c) AESO-NC3.

### 4.4. Biodegradability of the Nanocomposites

The degradation of polymers can proceed by one or more mechanisms, including microbial degradation in which microorganisms such as fungi and bacteria consume the material, macroorganism degradation in which insects and other macroorganisms masticate and digest the plastic, photodegradation in which exposure to ultraviolet radiation produces radical reactions and chain scission, and chemical degradation in which chemical reactions cleave bonds and reduce the molecular weight of the polymer. The degradation mechanisms can change depending on the polymer's environment and desired application.

In this part of the study, biodegradability studies of the renewable polymeric nanocomposites were focused on aerobic microbial degradation. Acrylated epoxidized soybean oil (AESO) is believed to be catabolized by microbes, but this process is slow and takes so much time. Biodegradability of the nanocomposites samples were studied by the soil burial method.

Weight loss of samples with different organoclay ratios was plotted as a function of time in Figure 4.21

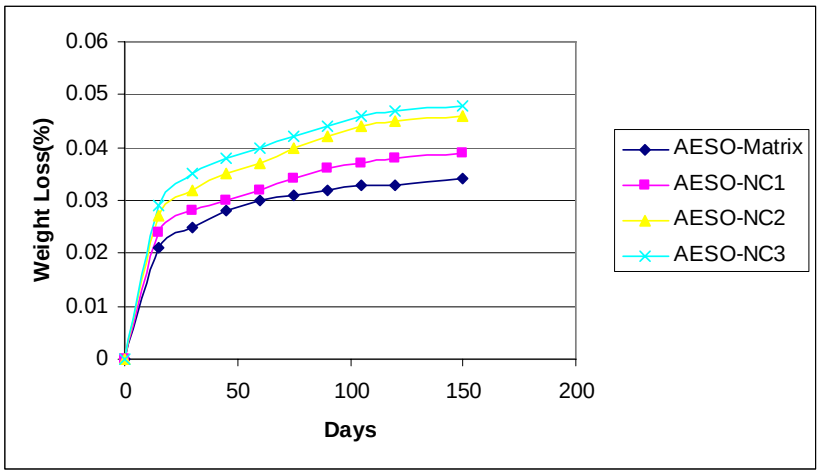


Figure 4.22 Weight loss vs. time curve for the nanocomposites

Weight loss was larger in nanoclay filled samples; the degradation was also directly proportional to clay content. Biodegradation rate increases with the increasing clay content in the nanocomposite most probably due to the existence of intercalant between the galleries as well as porosity leading to easy penetration of bacteria through the bulk of the material. All the samples have a large initial degradation rate and slow down later.

Scanning Electron Microscope (SEM) images were taken on the biodegraded surface of the renewable polymeric nanocomposites and polymer matrix under different magnifications. The samples with or without clay generates a similar degraded surface. In the Figure 4.23 and Figure 4.24, it can be seen that there are some pearl-like and shapeless structures on the biodegraded surfaces of the nanocomposites. These mostly ill-shaped structures on the surfaces of the nanocomposites are believed to be related to degradation by different microorganisms. Soil burial method shows that these nanocomposites have controlled biodegradation which makes these materials very attractive for biomedical and packaging applications.

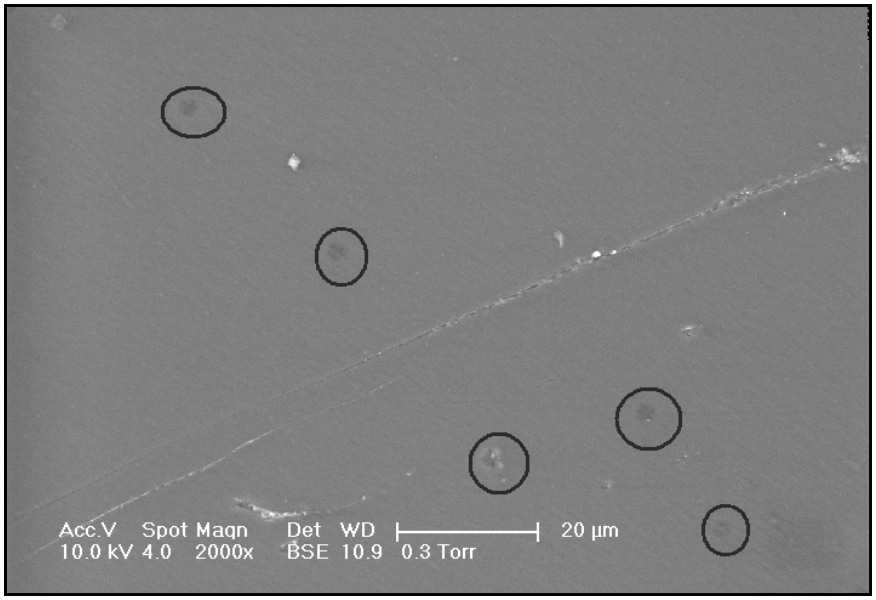


Figure 4.23 Low magnification SEM micrograph of the biodegraded nanocomposites

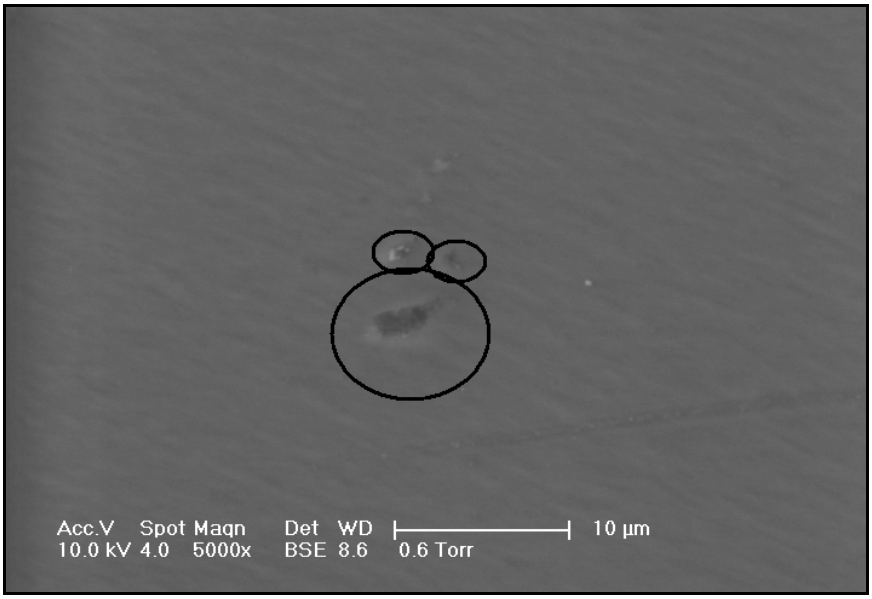


Figure 4.24 High magnification SEM micrograph of the biodegraded nanocomposites

### 4.5.Lysogeny Broth Studies of the Nanocomposites

Scanning Electron Microscope (SEM) images and optical microscope pictures were taken on the surface of the renewable polymeric nanocomposites and polymer matrix under different magnifications before and after the Lysogeny broth medium studies were carried out on these surfaces. It was found that resultant nanocomposites were not antibacterial and bacteria species could easily promote their growth on these nanocomposites. So, these results are consistent with the previous biodegradability studies' results which confirm the biodegradable properties of these nanocomposites. Promotion of bacteria species growth on nanocomposites' surfaces can be easily seen in the low and high magnification SEM images and optical microscope pictures (Figure 4.25 - Figure 4.27).

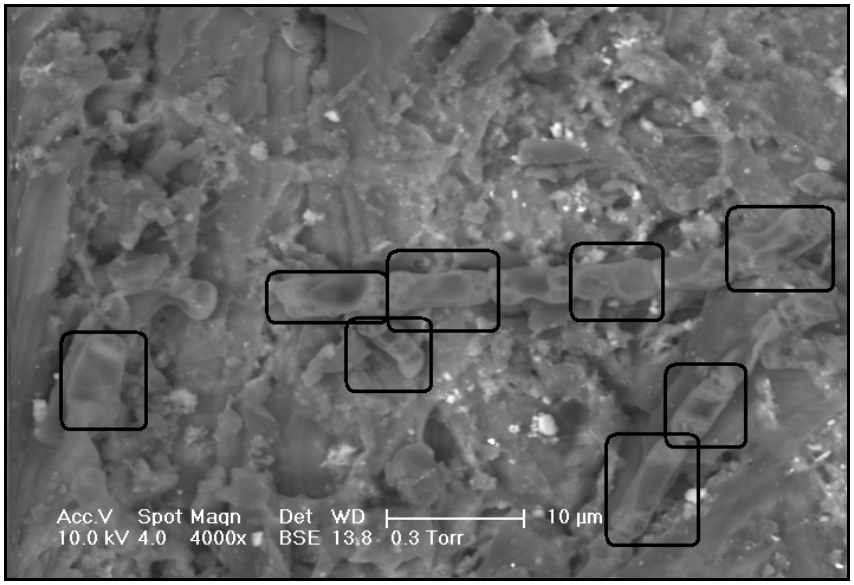


Figure 4.25 High magnification SEM micrograph nanocomposites after LB medium studies

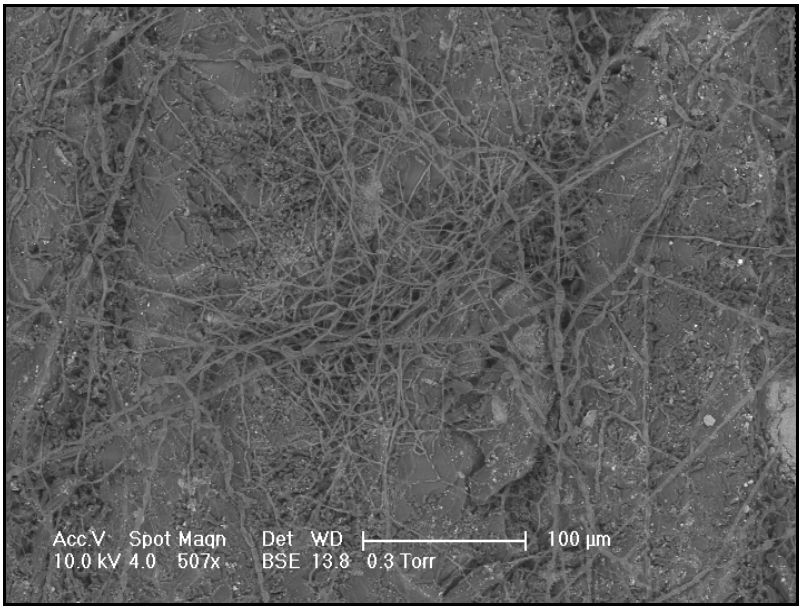


Figure 4.26 Low Magnification SEM Micrograph Nanocomposites After LB Medium Studies


Figure 4.27 Optical Microscope images of the Nanocomposites Before (a) and After (b) the LB Medium study

# 5. CONCLUSION

In this study, main purpose was to synthesize polymeric nanocomposites from renewable resources by using functionalized soybean oil based intercalant and matrix, and this aim was accomplished at the end of the study.

In the first part of the study, quarternized derivative of acrylated epoxidized soy bean oil (FA-Q-AESO) was synthesized to use it for modification of montmorillonite (MMT) clay. After synthesis of this bio-based renewable intercalant, FTIR (Fourier Transform Infrared) and NMR (Nuclear Magnetic Resonance) techniques were used to confirm synthesis of FA-Q-AESO. Modification of montmorillonite (MMT) clay was done with this bio-based renewable intercalant, and modification success was followed by X-ray diffraction (XRD) and Thermogravimetric Analysis (TGA) techniques. XRD data shows that there is an increase in interlayer spacing indicating an ordered intercalated system with the FA-Q-AESO modifier, so this renewable bio-based quarternized derivative of acrylated epoxidized soy bean oil works as an intercalant successfully. TGA data shows that there is a big difference in their degradation amounts which is directly related with the amounts of organic material which natural or modified MMT has in its structure. The degradation amounts results proved the success of modification, because organic part of the clay was increased in the modified montmorillonite (m-MMT). So, according to XRD and TGA data, montmorillonite (MMT) clay was successfully modified with quarternized derivative of acrylated epoxidized soy bean oil (FA-Q-AESO).

In the second part of the study, synthesis of renewable polymeric nanocomposites was completed by using AESO-S monomer solution and modified montmorillonite (FA-q-AESO-MMT). In-situ free radical polymerization technique was used in order to synthesize these nanocomposites, and polymeric nanocomposites from renewable resources with different nanoclay loadings were prepared. Then, all nanocomposites were characterized with X-ray diffraction (XRD), Atomic Force Microscopy (AFM), and Scanning Electron Microscopy (SEM) techniques to have information about their morphological properties. XRD analysis was used to identify nanocomposite structures, the absence of any peak in the diffractograms of all nanocomposite compositions indicates that the layer structure of the clays has been broken down and the clay platelets are well

separated from each other, so the clays are exfoliated. In all nanocomposite compositions, exfoliation structures were obtained. The extent of clay dispersion in the nanocomposites was also studied with atomic force microscopy (AFM). The phase images of the filled nanocomposites revealed the presence of clay plates as the bright features in the dark polymer matrix. A nanoscale dispersion of individual clay layers can be clearly observed in all loading degrees confirming the exfoliation structure as a good agreement with the facts shown in XRD patterns. Fracture surfaces of AESO-based matrix and its renewable bio-based polymeric nanocomposites were studied with Scanning Electron Microscopy (SEM) in order to obtain morphological properties of these polymeric materials. In the micrographs of the nanocomposites, it can be easily seen that nanocomposites have very smooth surfaces. It is evident from the micrographs that the morphology of the nanocomposites has a homogeneously dispersed phase of organoclays within the acrylated epoxidized soybean oil (AESO) matrix. This is in accordance with the X-ray diffraction (XRD) results.

In the third part of the study, the improvements in thermal and dynamic mechanical properties of the resultant nanocomposites and matrix were evaluated in terms of clay loading and extent of exfoliation by dynamic mechanical analysis (DMA), differential scanning calorimeter (DSC), and thermogravimetric analysis (TGA). The moduli of the all nanocomposites as well as tan delta peak temperatures are observed to be higher than that of the neat acrylated epoxidized soybean oil (AESO) matrix. Both shift and broadening of tan delta peak towards higher temperatures and increase in storage modulus values for the nanocomposites may be ascribed to their exfoliation morphologies with fine dispersion of organoclay layers in the polymer matrix leading to that provided a large aspect ratio for the clay, This increased polymer-clay interactions, making the entire surface area of the clay layers available for the polymer causing to restricted segmental motions near organic-inorganic interfaces and therefore leading to dramatic changes in the mechanical properties. TGA data of resulting nanocomposites were found to have significant improvements both in thermal and flame resistance properties with higher degradation onset temperatures and high char content. The onset degradation temperatures of all nanocomposites are higher than virgin matrix; moreover improvement reaches to almost 15 °C with only 2 % loading. The origin of this increase in the decomposition temperatures mainly results from the dispersed nanoscale silicate layers hindering the permeability of

the volatile degradation products out of the material resulting also in high char yields. DSC analysis was used to study the thermograms related with thermal transitions of pure matrix and nanocomposites. The effect of dispersed individual clay platelets on glass transition temperature (Tg) of matrix can be easily seen with the shift to higher temperatures indicating restricted segmental motions of polymer chains at the organic-inorganic interface due to the confinement of acrylated epoxidized soybean oil (AESO) polymer chains between the silicate layers as well as silicate surface-polymer interaction in nanostructure hybrids.

Finally, biodegradability studies of the nanocomposites and matrix was completed by using soil burial method. and it was found that all resultant nanocomposites were biodegradable in soil and it was found that increasing the clay content increase the biodegradability of the nanocomposites. In order to confirm biodegradability studies, Lysogeny broth medium was used, and it was found that resultant nanocomposites were not antibacterial and bacteria species could easily promote their growth on these nanocomposites.

# REFERENCES


1. Alexandre, M., and P. Dubois, "Polymer-Layered Silicate Nanocomposites: Preparation, Properties and Uses of a New Class of Materials", *Material Science and Engineering*, Vol. 28, pp. 1-63, 2000.

2. Ray, S.S., M. Okamato, "Polymer/ Layered Silicate Nanocomposites: A review from preparation to processing", *Progress in Polymer Science*, Vol.28, pp. 1539-1641, 2003.

3. Okada, A.,M. Kawasumi, A. Usuki, Y. Kojima, T. Kurauchi, and O. Kamigaito, "Nylon-6 Clay Hybrid", *Mater. Res. Soc. Proc*. Vol.171, pp. 45-50, 1990.

4. Theng, B.K.G., *The Chemistry of Clay-Organic Reactions*, New York: Wiley, 1974.

5. Hoffman, U., K. Endell, and D. Wilm, "Kristallstruktur and Quellung von Montmorillınit", *Z. Krist.* Vol.86, pp. 340-348, 1933.

6. Lagaly, G., "Interaction of Alkylamines with Different Types of Layered Compounds", *Solid State Ionics*, Vol. 22, pp. 43-51, 1986.

7. Şen, S., M. Memeşa, N. Nugay and T. Nugay, "Synthesis of Effective Poly(4-Vinylpyridine) Nanocomposites: In Situ Polymerization from Edges/Surfaces and Interlayer Galleries of Clay", *Polymer International*, Vol.55, pp.216-221, 2006.

8. Şen, S.,N. Nugay, and T.Nugay, "Structural Effects of Type of Intercalant in Poly(4-vinylpyridine) Nanocomposites: Compatible Homopolymer or Copolymer", *Polymer International,* Vol.55, pp.552-557, 2006.

9. Neşe, A., S. Şen, M.A. Taşdelen, N. Nugay, and Y. Yağcı, "Clay-PMMA Nanocomposites by Photoinitiated Radical Polymerization Using Intercalated Phenacyl Pyridinium Salt Initiator", *Macromol. Chem. Phys*. Vol.207, pp. 820-826, 2006.

10. Okada, A., A. Usuki, T. Kurauchi, and O. Kamigaito, "Polymer-Clay Hybrids, Hybrid Organic-Inorganic Composites", American Chemical Society, Vol. , pp.55-65, 1995.

11. Kojima, Y., A. Usuki, M. Kawasumi, A. Okada, T. Kurauchi, O. KAmigaito and K. Kaji, "Novel Preferred Orientation in Injection-Molded Nylon 6-Clay Hybrid", *J. Polym. Sci. Part B*, Vol.33, pp. 1039-1045, 1995.

12. Lemmon, J.P., J. Wu, C. Oriakhi and M.M. Lerner, "Preparation of Nanocomposites Containing Poly(ethylene oxide) and Layered Solids", *Electrochimica Acta*, Vol. 40, pp.2245-2249, 1995.

13. Biasci, L., M. Aglietto, G. Ruggeri and F. Ciardelli, "Functionalization of Monmorillonite by Methyl Methacrylate Polymers Containing Side-Chain Ammonium Cations", *Polymer*, Vol. 35, pp. 3296-3304, 1994.

14. Moet, A., A. Akelah, N. Salahuddin, A. Hiltner, and E. Baer, "Layered Silicate/ATBN Nanocomposite", *Mat. Res. Soc. Proc*., Vol.351, pp. 163-170, 1994.

15. Messersmith, P.B. and E.P. Giannelis, "Synthesis and Barrier Properties of Poly(ε-caprolactone)-Layered Silicate Nanocomposites", *J. Appl. Polym. Sci. Part A,* Vol. 33, pp. 1047-1057, 1995.

16. Vaia, R., A.H. Ishii and E.P. Giannelis, "Synthesis and Properties of Two-Dimensional Nanostructures by Direct Intercalation of Polymer Melts in Layered Silicates", *Chem. Mater*., Vol. 5, pp. 1694-1696, 1993.

17. Moet, A., A. Akelah, A. Hiltner, and E. Baer, "Layered Silicate/Polystyrene Nanocomposite", *Mat. Res. Soc. Symp. Proc*., Vol.351, pp.91-96, 1994.

18. Pinnavia, T. J., T. Lan, P. D. Kaviratna, and M. S. Wang, ”Clay-Polymer Nanocomposites: Polyether and Polyimides Systems”, *Mat. Res. Soc. Symp. Proc*., Vol.346, pp.81-87, 1994.

19. Yano, K., A. Usuki and A., Okada, “Synthesis and Properties of Polyimide-Clay Hybrid Films”, *J. Appl. Polym. Sci. Part A,* Vol.35, pp. 2289-2294, 1997.

20. Ke, Y., C. Long, and Z. Qi, “Crystallization, Properties and Crystal and Nanoscale Morphology of PET-Clay Nanocomposites”, *J. Appl. Polym. Sci.,* Vol. 71, pp. 1139-1146, 1999.

21. Lan, T. and T.J. Pinnavia, “Clay-Reinforced Epoxy Nanocomposites”, *Chem. Mater.* Vol. 6, pp. 2216-2219, 1994.

22. Kelly, P., A. Akelah, S. Qutubuddin, and A. Moet, “Reduction of Residual Stress in Montmorillonite/Epoxy Compounds”, *J. Mater. Sci.,* Vol. 29, pp. 2274-2280, 1994.

23. Messersmith, P.B. and E.P. Giannelis, “Synthesis and Characterization of Layered Silicate-Epoxy Nanocomposites”, *Chem. Mater*., Vol. 6, pp. 1719-1725, 1994.

24. Wang, Z., and T. J. Pinnavia, “Nanolayer Reinforcement of Elastomeric Polyurethane”, *Chem. Mater.,* Vol. 10, pp. 3769-3771, 1998.

25. Zilg,C., R. Thomann, R. Mulhaüpt, and J. Finter, “Polyurethane Nanocomposites Containing Laminated Anisotropic Nanoparticles Derived from Organophilic Layered Silicates”, Adv. Mater. Vol. 11, pp. 49-51, 1999.

26. Burnside, S. D., and E. P. Giannelis, “Synthesis and Properties of New Poly (dimethylsiloxane) Nanocomposites”, *Chem. Mater.,* Vol. 7, pp. 1597-1600, 1995.

27. Wang, S., C. Long, X. Wang, Q. Li, and Z. Qi, “Synthesis and Properties of Silicone/ Organo Montmorillonite Hybrid Nanocomposites”, *J. Appl. Polym. Sci.*, Vol. 69, pp.1557-1561, 1998.

28. Kornmann, X., *Synthesis and Characterization of Thermoset-Clay Nanocomposites*, PhD Thesis, Lulea University of Technology, 2001.

29. Pinnavia, T. J., and G. W. Beall, *Polymer Clay Nanocomposites*, Wiley Series in Polymer Science, John Wiley & Sons, 2000.

30. Weimer, M. W., H. Chen, E. P. Giannelis, and D. Y. Sogah, "Direct Synthesis of Dispersed Nanocomposites by In-situ Living Free Radical Polymerization Using a Silicate-anchored Initiator", *J. Am. Chem. Soc*., Vol. 121, pp. 1615-1616, 1999

31. Smith, A. K., and S. J. Circle, *Soybeans: Chemistry and Technology*, Westport, Connecticut, The Avi, 1972.

32. Küsefoğlu, S. H., R. Wool, G. Palmese, S Khot, and R. Zhoo, " High Modulus Polymers and Composites from Plant Oils", U. S. Patent No.6121398 (2000).

33. Williams, G. I., and R. P. Wool, "Composites from Natural Fibers and Soy Oil Resins", *Applied Comp. Mater*. Vol. 7, pp. 421-432, 2000.

34. O'Donnell, A., M. A. Dweib, and R. P. Wool, "Natural Fiber Composites with Plant Oil Based Resin", *Comp. Sci. & Tech*. Vol. 64, pp. 1135-1145, 2004.

35. Lu, J., C. K. Kong, and R. P. Wool, "Bio-based Nanocomposites from Functionalized Plant Oils and Layered Silicate", *Poly. Sci.*, Vol. 42, pp. 1441-1450, 2004.

36. Zhu, L., and R. P. Wool, "Nanoclay Reinforced Bio-based Elastomers: Synthesis and Characterization", Polymer, Vol. 47, pp. 8106-8115, 2006.

37. Lu, Y., and R. C. Larock, "Novel Bio-based Nanocomposites from Soybean Oil and Functionalized Organoclay", *Biomacromolecules*, Vol. 7, pp. 2692-2700, 2006.

38. Liu, Z., S. Z. Erhan, and J. Xu, "Preparation, Characterization and Mechanical Properties of Epoxidized Soybean Oil/ Clay Nanocomposites", *Polymer*, Vol. 46, pp. 10119-10127, 2005.

39. Liu, Z., and S. Z. Erhan, "Green Composites and Nanocomposites from Soybean Oil", *Mater. Sci. & Eng.,* Vol. 12, pp. 186-189, 2007.

40. Uyama, H., M. Kuwabara, T. Tsujimoto, M. Nakano, A. Usuki, and S. Kobayashi, "Organic-Inorganic Hybrids from Renewable Plant Oils and Clay", *Macromolecular Bioscience*, Vol. 4, pp. 354-360, 2004.

41. Kobayashi, S., H. Uyama, and T. Tsujimoto, "Green Nanocomposites from Renewable Resources: Biodegradable Plant Oil-Silica Hybrid Coatings", Macromol. Rapid Commun., Vol. 24, pp. 711-714, 2003.

42. Gohen, S. M., and R. P. Wool, "Degradation of Polyetylene-Starch Blends in Soil", *J. Appl. Poly. Sci*., Vol. 42, pp. 2691-2701, 1991

43. Bertani, G, "Studies on Lysogenesis", *J. Bacteriol.,* Vol. 62, 293-300, 1951

44. Landry, C.P.T., *Macromolecules,* Vol.26, pp 3702, 1993

45. Kojima, Y., Usuki, A., Kawasumi, M, Okada, A, Fukushima, Y, Karauchi, T, *J. Mater. Res*., Vol.6, pp 1185, 1993

46. Lu, J., Hong, C.K., and Wool, R.P., *J. Polymer Sci.,* Vol.42, pp 1441, 2004

47. Fu, X.A., Qutubiddin, S, Polymer, Vol. 42, pp 807, 2001

48. Suh, D.J., Lim, Y.T., Park, O.O., *Polymer*, Vol.41, pp 8557, 2000